Cooperative ring exchange and the fractional quantum Hall effect

Steven Kivelson,* C. Kallin,† Daniel P. Arovas,‡ and J. Robert Schrieffer
Institute for Theoretical Physics, University of California, Santa Barbara, California 93106
(Received 30 January 1987)

We study the transition of the interacting two-dimensional electron gas at high magnetic field from a low-density Wigner crystal to a higher-density correlated state which exhibits the fractionally quantized Hall effect. The phase transition is precipitated by a condensation of ring-exchange processes, which by nature of their sensitivity to enclosed magnetic flux allow for especially low-energy exchange condensates at certain values of the Landau-level filling factor, $\nu=\nu_i$. In the condensate, the exchanges mediate a logarithmic potential between local-density fluctuations, leading to a cusp in the ground-state energy as a function of $|\nu-\nu_i|$ in the vicinity of a preferred state. In addition, we derive quasiparticle excitations of sharp fractional charge which are analogous to the excitations derived by Laughlin.

I. INTRODUCTION

The remarkable discovery of anomalies in the transport properties of a two-dimensional (2D) electron or hole gas in a strong magnetic field at integral[1] and fractional[2] filling ν of the lowest Landau level has stimulated considerable theoretical activity. In particular, in semiconductor heterojunctions it is observed that the Hall conductivity σ_{xy} exhibits plateaus at integer filling factors $\nu_i=1,2,\ldots$, as well as at rational values of ν_i with odd denominators, e.g., $\nu_i=\frac{1}{3},\frac{1}{5},\frac{2}{5},\ldots$, with σ_{xy} quantized very accurately to values $\nu_i e^2/h$. In addition, the longitudinal resistance ρ_{xx} is observed to become extremely small near ν_i. While the integer effect can in essence be accounted for within the context of one-body theory, the fractional quantum Hall effect (FQHE) is fundamentally a consequence of many-body correlations.

Most theoretical attempts to account for the FQHE are based on the following general picture.[3,4] Near certain filling factors ν_i the energy $E(\nu)$ of the system is particularly low, exhibiting cusplike behavior at each ν_i. As a consequence, at these cusps the chemical potential $\mu=dE/d\nu$ is discontinuous, corresponding to a gap $2\Delta=(e^*/e)(\mu_+-\mu_-)$ in the spectrum for creating a pair of widely spaced quasiparticle excitations of charge e^*. In the presence of defects, added charge $\delta\nu=\nu-\nu_i$ becomes pinned at the defects, causing σ_{xy} to be constant near ν_i. For large $\delta\nu$ the defects are saturated and the unbound added charge enters the condensate increasing its density toward its value at the next plateau. Presumably, the minimum of ρ_{xx} at ν_i is also a consequence of the gap 2Δ, with intrinsic dissipation being thermally activated. On the basis of this picture, a number of approaches have been advanced to account for the origin of the cusps as well as the nature of the low-lying excitations.

Early theoretical attempts focused on a Hartree-Fock approach to the 2D electron gas in a strong magnetic field B.[5-8] Within this approximation, it was shown that E is a smooth function of ν, without cusps. The first successful theory of the FQHE was proposed by Laughlin.[9] Working in the symmetric gauge $\mathbf{A}=\frac{1}{2}\mathbf{B}\times\mathbf{r}$, with $\mathbf{B}$ in the direction normal to the 2D (x,y) plane, he assumed the electronic ground state for a fractional filling factor $\nu=1/m$ is well approximated by a Jastrow-type function,

$$\Psi_0=\mathcal{N}_0\prod_{\substack{j,k\\(j<k)}}(z_j-z_k)^m\exp\left[-\tfrac{1}{4}\sum_l|z_l|^2/l^2\right], \tag{1.1}$$

where $l=(\hbar c/eB)^{1/2}$ is the magnetic length. Here $z_j=x_j+iy_j$ is the complex one-electron coordinate. To satisfy the Pauli exclusion principle and to ensure that only states in the lowest-energy Landau level are involved, m must be an odd integer. As Haldane and others[10,11] have discussed, for a class of short-range potentials, the Laughlin-Jastrow function (1.1) is the exact ground state for $\nu=1/m$.

To describe a quasihole located at complex coordinate z_0, Laughlin proposed the state

$$\Psi_1=\mathcal{N}_1\prod_i(z_i-z_0)\Psi_0\ . \tag{1.2}$$

The factor z_i-z_0 raises the angular momentum of electron i, measured about z_0, by the amount $+1$, leaving a region of reduced electron density at z_0. Since the mean density per quantum of flux is ν, the charge of the quasiparticle is $e^*=\nu e$, a fractional value. This is the analog of fractionally charged solitons in one-dimensional systems.[12] While a factor $(z_i-z_0)^\alpha$ for noninteger α would give charge $\alpha\nu e$, only integer α is allowed if one is to remain in the lowest Landau level. For $\nu=\frac{1}{3}$ (and $\alpha=1$), Laughlin estimates the quasihole creation energy to be $\Delta_-=0.026e^2/\epsilon l$.

The quasielectron is obtained by lowering the angular momentum of each electron, thereby increasing the electron density near the origin. Similar arguments to those above lead to a charge $-\nu e$ and a creation energy, which Laughlin estimated to be $\Delta_+=0.030e^2/\epsilon l$ for $\nu=\frac{1}{3}$. It has been suggested that these excitations obey fractional statistics.[13,14]

Based on these results, Laughlin argued that the state describes an incompressible system in that ν can be changed by a small amount $\delta\nu$ only if the extra charge is added in the form of quasiparticles. Therefore, the energy increase near ν_i is linear in $\delta\nu$, $\delta E = N \mid \delta\nu \mid \Delta$, where N is the number of flux quanta in the area A of the system. In a compressible system, δE is quadratic in $\delta\nu$ and therefore the system exhibits gapless sound waves or magnetophonons.

Extensive numerical calculations[15–17] have been carried out for small numbers of electrons to investigate the ground state and excitations of an interacting electron gas in a strong magnetic field. Haldane and Rezayi[15] have recently studied up to eight electrons in a spherical geometry for filling factor $\nu=\frac{1}{3}$, using a Coulomb potential. Remarkably, for six electrons, the projection of their fully diagonalized state on the Laughlin-Jastrow state is over 99%.

To investigate the excitation spectrum Girvin, MacDonald, and Platzman[18] used an approach similar to that of Feynman[19] for ^{4}He. In this scheme one considers the Fourier component $\rho_{\mathbf{k}}$ of the density operator suitably projected onto the lowest Landau level. When this operator is applied to the ground state, one assumes that most of the weight arises form a single mode. Using the oscillator strength sum rule and the structure factor $S(\mathbf{k})$ obtained form the Laughlin-Jastrow function, one finds a spectrum which exhibits a gap for all $\mathbf{k}$, reflecting the incompressibility of the system. In addition, these authors find a magnetoroton minimum analogous to the roton minimum in ^{4}He.

The above discussion has been limited to the "fundamental" steps, $\nu=1/m$, where m is an odd integer. To account for steps at densities n/m where n differs from 1 and from $m-1$, Haldane,[10] Halperin,[14] and Laughlin[20] proposed a hierarchy of condensates, each step of the hierarchy being formed from the quasiparticles of the preceeding step. While giving a good qualitative description of the n/m steps, the mean spacing between quasiparticles is comparable to their intrinsic size, making a detailed theory of this approach difficult.

Laughlin's ground state appears to be a remarkably good approximation to the exact ground state. However, it is not clear which of the correlations that are built into Laughlin's wave function are essential for the fractional quantum Hall effect, and what their physical origin is. On the one hand, the fact that this wave function keeps the electrons well apart at short distances appears to be very important. On the other hand, Laughlin's wave function builds in strong correlations between the position of one electron and the positions of all other electrons. Moreover, the incompressibility which characterizes the quantum-Hall ground state, is a long-wavelength collective property of the system. In particular, it is an interesting open question whether or not an order parameter which exhibits long-range or quasi-long-range order can be defined for the system.[21,23] By adopting a fresh approach to this problem, we believe that we can shed some light on these issues.

The present work has as its point of departure the low-density limit investigated by Maki and Zotos.[8] As $\nu\rightarrow 0$ (or $\mid 1-\nu \mid \rightarrow 0$) the electrons (or holes) form a Wigner lattice. Corrections to the zeroth-order Madelung energy arise from lattice vibrations and pairwise exchange. These energies are smooth functions of ν. Maki and Zotos calculated the contribution to E from exchanges involving a triangle of three electrons. They treated the problem as two pairwise exchanges and found an energy lowering when the Wigner and magnetic lattice periods are commensurate. Unfortunately, the magnitude of the effect was found to be 4 orders of magnitude too weak and a flat minimum rather than a cusp was found at densities $\nu=1/m$, where m is an odd integer. It is clear that the Aharonov-Bohm phase is what leads to this effect,[24] although it is difficult to see how one can obtain the required cusps or the correct order of magnitude of the strength of the cusps from this argument alone. As we will discuss, the phenomenon is a rather subtle one.

It is not even *prima facie* clear whether exchange processes should be expected to lower the ground-state energy, and hence produce a particularly stable ground state when they add in phase, or in fact raise the energy. In the absence of a magnetic field, the antisymmetric ground state always has higher energy than the unsymmetrized ground state—exchange always raises the energy of a fermion system. This is because exchange builds nodes into the wave function and, hence, increases the ground-state kinetic energy. However, in a strong magnetic field, the kinetic energy is quenched. In this case, the dominant effect of exchange can be to reduce the repulsive interaction between electrons. Hence, exchange can indeed lower the ground-state energy.

In a recent paper[24] we proposed an explicit mechanism whereby exchange processes can lead to cusps in the ground-state energy. Furthermore, we showed how the quasiparticle charge is quantized in this approach. The basic idea is that rings of electrons undergo *cooperative* tunneling processes in which each particle moves to the site initially occupied by one of its neighbors. It is this tunneling current when coupled to the vector potential $\mathbf{A}$, through the Aharonov-Bohm effect, which leads to coherent superposition of the exchange energies from all rings when the flux inside each ring is a multiple of the flux quantum. The sharpness of the cusps arises from the importance of large rings, which are extremely sensitive to changes of density. The large overall magnitude of the effect is due to the low tunneling barrier which arises from the fact that the electrons are moving cooperatively along the tunneling path.

In essence, as the density increases, the number of ring tunneling events per unit time increases until the system passes through a phase transition, after which the system is filled with rings. These rings enter with arbitrary phase except near critical values of the density given by rational values n/m, where they add in phase, lowering the energy in a cusplike form. Quasiparticles are formed, much as in the Laughlin theory, and have their charge quantized by the fact that charges other than the proper values have infinite energy.

Recently, Baskaran[25] has argued that the cooperative ring-exchange mechanism need not be tied to the Wigner crystal, but may be defined relative to the typical

configuration of an incompressible fluid. While we are not sure this problem has been completely resolved, we also feel that the crystalline lattice is not an essential feature of the theory described in this paper. We will return to this point in the conclusions.

This paper provides a detailed analysis of the theory put forward in our earlier Letter[24] and also includes new results on the excitations. The structure of the paper is as follows. In Sec. II we discuss the path-integral formulation of the problem and the coherent-state basis. The essential role played by cooperative ring-exchange processes is deduced and the contribution from various types of exchange paths is discussed. In Sec. III the problem of summing over all cooperative ring-exchange contributions is mapped onto the discrete Gaussian model, and in turn onto the Coulomb gas, whose properties are largely known. This leads to a ground-state energy exhibiting cusps of the form $|\delta\nu|\ln|\delta\nu|$, which motivates the need for quasiparticles.

Quasiparticle excitations are deduced in Sec. IV where it is shown that the condition that all exchange rings add coherently leads to fractional charge quantization. Boson excitations (collective modes) are also discussed. A summary, remarks and conclusions are given in Sec. V. In addition, there are six appendices. A discussion of how exchange processes can lower the energy of a fermion system in a strong magnetic field is contained in Appendix A. Appendixes B and C contain the formalism necessary in deriving a coherent-state path-integral expression for the partition function. Appendix D contains some details of the calculation of the classical action, Appendix E reviews some of the statistical mechanics of certain models that we use, and Appendix F contains a lowest-order calculation of the magnetophonon spectrum in the dense exchange phase.

II. PATH-INTEGRAL FORMULATION

A. Coherent-state path integral

One can develop a path-integral formulation for a two-dimensional system of electron confined to the lowest Landau level by using a coherent-state representation.[26,27] We use such a formulation to calculate the partition function $Z(\nu)$ for the partially filled Landau level in the steepest-descent or saddle-point approximation. The ground-state energy is then obtained from the partition function as

$$E(\nu)=-\lim_{\beta\to\infty}\frac{1}{\beta}\ln Z(\nu)\ ,$$

where β is the inverse temperature.

The partition function for a two-dimensional system of N electrons in a perpendicular magnetic field $\mathbf{B}=-B_0\hat{\mathbf{z}}$ may be written as

$$Z(\nu)=\mathrm{Tr}\,e^{-\beta H}=\frac{1}{N!}\sum_{\sigma\in S_N}\mathrm{sgn}(\sigma)\int\prod_{k=1}^{N}d^2r_k\langle\mathbf{r}_1,\ldots,\mathbf{r}_N\,|\,e^{-\beta H}\,|\,\mathbf{r}_{\sigma(1)},\ldots,\mathbf{r}_{\sigma(N)}\rangle\ , \tag{2.1}$$

where the sum is over all permutations σ and, in the symmetric gauge,

$$H=\sum_{i=1}^{N}\left[\frac{1}{2m^*}\left[\mathbf{p}_i+\frac{e}{2c}B_0\hat{\mathbf{z}}\times\mathbf{r}_i\right]^2+U_1(\mathbf{r}_i)+\sum_{j(<i)}V_2(\mathbf{r}_i-\mathbf{r}_j)\right]\ . \tag{2.2}$$

Here, $V_2(\mathbf{r})=e^2/\epsilon r$ is the Coulomb potential and U_1 is the interaction with the neutralizing background. In the limit that the splitting between Landau levels, $\hbar\omega_c=\hbar eB/m^*c$, is much greater than the Coulomb energy ($m^*\to 0$), we can project the Hamiltonian onto the lowest Landau level. This results in an expression for Z as a path integral over an overcomplete basis of direct-product single-electron coherent states $|\mathbf{R}\rangle$ which span the lowest Landau level. The position-space representation of $|\mathbf{R}\rangle$ is

$$\phi_{\mathbf{R}}(\mathbf{r})=\langle\mathbf{r}\,|\,\mathbf{R}\rangle=(2\pi)^{-1/2}\exp\left[-\tfrac{1}{4}|\mathbf{r}-\mathbf{R}|^2+\frac{i}{2}(\mathbf{r}\times\mathbf{R})\cdot\hat{\mathbf{z}}\right], \tag{2.3}$$

where we set $l=\sqrt{\hbar c/eB}\equiv 1$. [Henceforth, we will adopt the notation $\mathbf{a}\wedge\mathbf{b}\equiv(\mathbf{a}\times\mathbf{b})\cdot\hat{\mathbf{z}}$ for two-dimensional cross products.] The general properties of these coherent states are reviewed in Appendix B. We stress that the state label $\mathbf{R}$ is a continuous quantity. The overlap between two such states is given by

$$\langle\mathbf{R}_1\,|\,\mathbf{R}_2\rangle=\exp\left[-\tfrac{1}{4}|\mathbf{R}_1-\mathbf{R}_2|^2+\frac{i}{2}\mathbf{R}_1\wedge\mathbf{R}_2\right]\ . \tag{2.4}$$

The derivation of the discrete-time path integral proceeds in the usual way, as discussed in Appendix C, and one obtains

$$Z(\nu)=\mathcal{N}\sum_{\sigma\in S_N}\mathrm{sgn}(\sigma)\int\prod_{j=1}^{N}\prod_{n=0}^{M}d\mathbf{R}_j(n\varepsilon)e^{-S[\mathbf{R}]}\ , \tag{2.5}$$

where $\mathcal{N}$ is a normalization constant, $\mathbf{R}_j(n\varepsilon)$ labels the center of the coherent state occupied by particle j at (imaginary) time $\tau=n\varepsilon$, $\varepsilon=\beta/M$, and, from the definition of the trace, the $\mathbf{R}_j$ satisfy the boundary conditions

$$\mathbf{R}_j(0)=\mathbf{R}_{\sigma(j)}(\beta)\ . \tag{2.6}$$

The action function in Eq. (2.5) is

$$S[\mathbf{R}]=\sum_{n=0}^{M}\left[\sum_{j=1}^{N}\{-\tfrac{1}{2}[\mathbf{R}_j(n\varepsilon+\varepsilon)-\mathbf{R}_j(n\varepsilon)]\cdot[\mathbf{R}_j(n\varepsilon)+i\mathbf{R}_j(n\varepsilon)\times\hat{\mathbf{z}}]+\varepsilon U_j(n\varepsilon)\}+\varepsilon\sum_{\substack{j,k\\(j<k)}}^{N}V_{jk}(n\varepsilon)+O(\varepsilon^2)\right], \tag{2.7}$$

where

$$V_{jk}(\tau)=\frac{\langle\mathbf{R}_j(\tau)\mathbf{R}_k(\tau)\,|\,V_2\,|\,\mathbf{R}_j(\tau+\varepsilon)\mathbf{R}_k(\tau+\varepsilon)\rangle}{\langle\mathbf{R}_j(\tau)\mathbf{R}_k(\tau)\,|\,\mathbf{R}_j(\tau+\varepsilon)\mathbf{R}_k(\tau+\varepsilon)\rangle}\ . \tag{2.8}$$

The discrete-time path integral in Eq. (2.5) is well defined for time step ε small but nonzero. The integration over the variables X_j and Y_j in each time slice can be performed along any contour in the complex X_j and Y_j planes that runs from $-\infty$ to $+\infty$. In general, the continuum limit ($\varepsilon\to 0$) of Eq. (2.5) is fraught with mathematical difficulties because of the existence of discontinuous paths with finite action. One can handle this difficulty either by keeping ε nonzero at all intermediate steps of the calculation, or by considering the usual Feynman (Weiner) path integral for the partition function and taking the limit $m^*\to 0$ at the end.[27] (These subtleties are inconsequential for calculating the classical action, but can be important for calculating the sum over paths in the vicinity of the classical path i.e., the fluctuation determinant.) Despite these difficulties, the continuum version of the path integral can be used to develop a saddle-point approximation for the partition function,[27,28] as discussed in the next section. In this case, Eqs. (2.5) and (2.7) become

$$Z(\nu)=cN\sum_{\sigma}\mathrm{sgn}(\sigma)\int\prod_{j=1}^{N}\mathcal{D}\mathbf{R}_j(\tau)e^{-S[\mathbf{R}(\tau)]}\ , \tag{2.9}$$

$$S[\mathbf{R}]=\int_0^{\beta}d\tau\left[\sum_{j=1}^{N}\left[-\frac{i}{2}\dot{\mathbf{R}}_j\wedge\mathbf{R}_j+U(\mathbf{R}_j)\right]+\sum_{\substack{j,k\\(j<k)}}V(\mathbf{R}_j-\mathbf{R}_k)\right], \tag{2.10}$$

where $U(\mathbf{R})=\langle\mathbf{R}\,|\,U_1\,|\,\mathbf{R}\rangle$ is the neutralizing background term and V is the matrix element of the Coulomb potential between coherent states,

$$V(\mathbf{R})=\frac{\sqrt{\pi}e^2}{2\epsilon}e^{-R^2/8}I_0(R^2/8)\ . \tag{2.11}$$

B. Saddle-point approximation

Having formulated the problem in terms of a path integral, we proceed to evaluate it within the saddle-point (or semiclassical) approximation. For the class of paths which we consider, there is a single quantum parameter, which we will call $g/8\pi$, which is simply proportional to the ratio of the extent of the electron wave packet due to its zero-point motion to the mean area per electron. Hence, $g/8\pi$ is proportional to ν and, as one would expect, the semiclassical approximation is valid at low electron densities where the ground state is believed to be a Wigner crystal. In fact, we shall see that $g/8\pi<0.1$ for $\nu<\frac{1}{2}$, and therefore this approximation is possibly justified at intermediate densities as well.

In the saddle-point approximation the path integral is evaluated by a multidimensional version of the method of steepest descents. Thus our prescription is to first find all those paths $R^c(\tau)$ which extremize the action, $\delta S/\delta\mathbf{R}_j(\tau)\,|_{R=R^c}=0$. [$R^c$ is a vector function with $2N$ components $\mathbf{R}_j(\tau)$ which we will call a "classical" path. It is important to keep in mind, however, that $\mathbf{R}_j(\tau)$ labels the center of a coherent state, i.e., it is a guiding-center coordinate and not the coordinate of a point electron.] The path integral can then be expressed as a sum over saddle-point contributions in which the contribution of paths in the neighborhood of each classical path is evaluated by expanding the action to quadratic order in $R-R^c$. In this way Z can be expressed in terms of a sum over classical paths (assuming them to be well separated in path space)

$$Z=\sum_c e^{-S[R^c]}D[R^c]\ , \tag{2.12}$$

where $S[R^c]$ is the action evaluated along the classical path (and includes a phase factor arising from Fermi statistics) and $D[R^c]$ is the fluctuation determinant.

It follows from the discrete-time equations of motion that the classical (extremal) paths are continuous, except possibly at the endpoints (see Appendix C) and therefore can also be derived from the continuous time action. The classical paths satisfy the equations of motion:

$$i\dot{X}_j=\frac{\partial V}{\partial Y_j},\quad i\dot{Y}_j=-\frac{\partial V}{\partial X_j}\ , \tag{2.13}$$

where $V\equiv\sum_{i<j}V(\mathbf{R}_i-\mathbf{R}_j)$. These are simply the imaginary-time $\mathbf{E}\times\mathbf{B}$ drift equations, which have the property that a classical path lies along an equipotential contour $\dot{V}=0$. In addition, the classical paths satisfy the boundary conditions given in Eq. (2.6). As is usual in the saddle-point approximation, each variable (in this case, each X_j and Y_j) is analytically continued into the complex plane in the search for saddle points, while the initial and final values remain real and fixed. This is done by deforming the contour of integration in each time step so that it passes over the saddle point in the direction of steepest descent.[28] In the present case, the classical paths may be discontinuous at the endpoints. This results from the fact that it is not always possible to find solutions to the classical equations of motion, which are first-order equations, that also satisfy both the initial and final

boundary conditions. In this case one obtains an additional contribution to the classical action from the discontinuities at the endpoints.[27] However, for the specific paths which we will consider, the endpoint contributions to the action are negligible. (See Appendix C.)

By making the coordinate change $\mathbf{R}=R-R^c$ we can express the fluctuation determinant $D[R^c]$ as a path integral of the same form as that in Eqs. (2.5)–(2.7) but with the potential $V\equiv\sum_{i<j}V_{ij}$ in Eq. (2.7) replaced by the time-dependent quadratic potential:

$$V\rightarrow\tfrac{1}{2}\sum_{i,j}(X_iK_{ij}X_j+X_iL_{ij}Y_j+Y_iL_{ij}X_j+Y_iW_{ij}Y_i)\ , \tag{2.14}$$

where

$$K_{ij}(R^c)=\left.\frac{\partial^2V_{ij}}{\partial X_i\partial X_j}\right|_{R=R^c(\tau)}\ ,$$
$$L_{ij}(R^c)=\left.\frac{\partial^2V_{ij}}{\partial X_i\partial Y_j}\right|_{R+R^c(\tau)}\ , \tag{2.15}$$
$$W_{ij}(R^c)=\left.\frac{\partial^2V_{ij}}{\partial Y_i\partial Y_j}\right|_{R=R^c(\tau)}\ .$$

From the relation of Eq. (2.5) to the phase-space path integral it is clear that $D[R^c]$ is the partition function for a set of N coupled harmonic oscillators with time-dependent coupling constants:

$$D[R^c]=\mathrm{Tr}T\left[\exp\left[-\int_0^\beta d\tau\,H(R^c(\tau))\right]\right]\ , \tag{2.16a}$$

where T is the time-ordering operator,

$$H(R^c)=\tfrac{1}{2}\sum_{i,j}[P_iW_{ij}(R^c)P_j+P_iL_{ij}(R^c)X_j+X_iL_{ij}(R^c)P_j+X_iK_{ij}(R^c)X_j]\ , \tag{2.16b}$$

and $[P_j,X_j]=-i\delta_{jk}$.

Let us begin to classify the classical paths. The path with the smallest action is a stationary path, the triangular Wigner crystal. This path and Gaussian fluctuations about it make the dominant contribution to the partition function $D_0e^{-S_0}=\exp[-\beta NE_0(\nu)]$, where $E_0(\nu)$ is the energy per site of the static Wigner crystal, which is essentially the Hartree energy that has been computed by Maki and Zotos.[8] The contribution to this energy from pair exchange can also be calculated by using the discrete-time version of the path integral. $E_0(\nu)$ is a smooth, monotonic function of ν for $\nu<\frac{1}{2}$. Maki and Zotos also noted that for $\nu>\nu_+\approx 0\,45$ the Wigner crystal is classically unstable since the shear modulus is negative. Thus we must confine ourselves to $\nu<\nu_+$. (For $\nu>1-\nu_+$, the same considerations apply for the hole lattice.)

All other classical paths apparently have action larger than S_0; however, there are very many of them. We assume that, so as not to have prohibitively large action, the important classical paths resemble the Wigner crystal at most points in space, most of the time. We will return to this assumption later. In this case, it is convenient to rewrite the sum in Eq. (2.12) in a form that allows us to focus on the difference between a particular classical path and the static Wigner crystal

$$Z=D_0e^{-S_0}\sum_c\tilde{D}[R^c]e^{-\tilde{S}[R^c]}\ , \tag{2.17}$$

where $\tilde{D}=D/D_0$ and $\tilde{S}=S-S_0$.

C. Cooperative ring-exchange paths

We now focus on those paths which are most likely to lead to structure in $E_c(\nu)$ because of their systematic dependence on ν. That is, we consider paths, such as those illustrated in Fig. 1, which consist of a cyclic coherent superposition of nearest-neighbor exchanges from the initial static Wigner crystal configuration. Each such exchange event can be characterized by a directed path on the Wigner lattice, as shown in the figure, and by the time $0<\bar{\tau}<\beta$ at which the event occurs. Paths involving second- or further-neighbor exchanges (see Fig. 2) have larger real parts of the action (not only because the electrons must tunnel larger distances but also because the electrons come closer together along the path and hence must tunnel through larger potential barriers) and are therefore neglected.

Let us consider the contribution to the reduced partition function $\tilde{Z}$ from a single large ring exchange involving L electrons. The classical action, from Eq. (2.12), is

$$\tilde{S}[R^c]=-\frac{i}{2}\sum_{j=1}^{N}\int_0^\beta dr\,\dot{\mathbf{R}}_j^c\wedge\mathbf{R}_j^c+i\pi(L-1)\ , \tag{2.18}$$

where $\mathbf{R}_j^c$ satisfies the equations of motion, Eq. (2.13), with the potential $\tilde{V}\equiv\sum_{i<j}[V(\mathbf{R}_i-\mathbf{R}_j)-V(\mathbf{R}_i^0-\mathbf{R}_j^0)]$, and $\mathbf{R}_j^0=\mathbf{R}_j^c(\tau=0)$ is the position of the jth electron in the initial static Wigner crystal configuration. It follows from the equations of motion that along the classical path the potential $\tilde{V}$ is zero. The term $i\pi(L-1)$ in Eq. (2.18) reflects the Fermi statistics. If the electrons involved in the ring exchange are labeled from 1 to L, then the R_j^c satisfy the following boundary conditions:

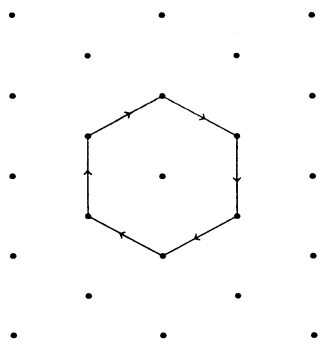

FIG. 1. An example of a cooperative ring-exchange path.

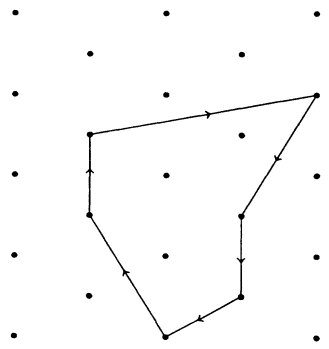

FIG. 2 A ring-exchange path involving further-neighbor exchanges. This six-particle exchange process is of a substantially smaller amplitude than that depicted in Fig. 1.

$$\begin{aligned}&\mathbf{R}_1^c(\beta)=\mathbf{R}_L^c(0)\ ,\\&\mathbf{R}_{j+1}^c(\beta)=\mathbf{R}_j^c(0),\quad j=1,\ldots,L-1\\&\mathbf{R}_j^c(\beta)=\mathbf{R}_j^c(0),\quad j \text{ not on the ring}\ .\end{aligned}\tag{2.19}$$

The real part of the action is approximately proportional to L, since each electron tunnels through a similar barrier, and the imaginary part, from Eqs. (2.18) and (2.19), is[29]

$$\begin{aligned}&\theta=-\tfrac{1}{2}\sum_{j=1}^{L}\int_0^\beta d\tau\,\dot{\mathbf{R}}_j^{c'}\wedge\mathbf{R}_j^{c'}+\pi(L-1)\ ,\\&\theta=\pm 2\pi(\phi/\phi_0)+\pi(L-1)\ ,\end{aligned}\tag{2.20}$$

where $\mathbf{R}_j^{c'}$ is the real part of $\mathbf{R}_j^c$, ϕ is the flux enclosed by the path, and the $\pm$ refers to positive or negative sense of rotation. The first term in Eq. (2.20) is the phase from the Aharonov-Bohm effect. If the classical path exactly followed the straight-line segments between sites (as shown in Fig. 1) then one would have $\phi/\phi_0=N_A/2\nu$, N_A is the number of enclosed plaquettes of area $\Omega_\nu\equiv\pi l^2\nu$. In this case, the phase would be

$$\theta=\pm\pi\left[\frac{1}{\nu}-1\right]N_A+\pi\pmod{2\pi}\ ,\tag{2.21}$$

where we have used the fact that, for the triangular lattice, N_A is odd (even) when L is odd (even). Similarly, the real part of the action would be $\alpha_0(\nu)L$, where α_0 is independent of path.

In fact, due to the presence of corners, the classical paths do not follow precisely straight-line segments, α_0 is not independent of path, and for any particular single ring exchange there are corrections to the phase expressed in Eq. (2.21). We will argue that the net effect of such corrections is to renormalize α_0, but first let us consider the fluctuation determinant.

The important contributions to the reduced fluctuation determinant $\tilde{D}[R^c]$ come from those regions of space and time where R^c differs appreciably from a Wigner crystal. From Eq. (2.16), this implies that

$$\tilde{D}[R^c]=-(\cdots)\frac{d\tau}{\tau_0}e^{-\Delta\alpha(\nu)L}\ ,\tag{2.22}$$

where $\Delta\alpha$ is a real constant which acts to renormalize α_0 and τ_0 is the characteristic tunneling time. As in all instanton calculations, by constraining the exchange to occur at time $\bar{\tau}$, we break time-translation invariance. Therefore, in obtaining an expression for $\tilde{D}[R^c]$ from Eq. (2.16), the resulting zero mode is suppressed and instead an explicit integral over the flip time is included, as represented by the factor $d\tau/\tau_0$. We have not explicitly calculated the prefactor, which is denoted by $(\cdots)$ in Eq. (2.22), for a general classical path. (The calculation of $\tilde{D}$ for an especially simple path is discussed below in Sec. II D.) We can at best estimate the leading order contribution of large cooperative ring exchanges ($L\to\infty$) to $\ln Z(\nu)$. Corrections that are sublinear in L (i.e., there are $\ln L$ corrections from the prefactor) are too subtle to be included at the present level of approximation. However, the phase of the prefactor is important and must be correctly calculated. In Appendix A we argue that the fluctuation determinant is real and negative.

The results of Eqs. (2.21) and (2.22) can be summarized as

$$\tilde{D}[R^c]e^{-\tilde{S}[R^c]}=\frac{d\tau}{\tau_0}\exp[-\alpha(\nu)L\pm i2\pi fN_A+O(\ln L)]\ ,\tag{2.23}$$

where $\alpha=\alpha_0+\Delta\alpha$ and $f=\frac{1}{2}[(1/\nu)-1]$. It is apparent from Eq. (2.23) that when ν^{-1} is an odd integer, the contribution from different ring exchanges will add in phase. Although the contribution from a given large ring exchange is exponentially small, the number of ring exchanges involving L electrons also grows exponentially. Thus when the tunneling coefficient $\alpha(\nu)$ is sufficiently small, arbitrarily large ring exchanges will contribute to the energy, and when their phases are such that the different contributions add coherently, then a particularly stable ground state is found. This phase relation is also preserved when some further-neighbor exchanges are considered, and we do not expect the inclusion of such exchanges (which we have neglected) to change the results qualitatively.

One feature of the classical path which is worth noting is that the characteristic time τ_0 over which the electrons are actually moving is determined by local interactions and so is roughly independent of the length of the exchange loop. Moreover, as is typical for tunneling paths, the motion is exponentially localized in time so that interactions between exchange events that are separated by a time interval greater than τ_0 are negligible.

In deriving Eq. (2.23) we have assumed that the classical paths were constructed from L straight-line segments between the lattice points so that the enclosed area A is an integral multiple of the plaquette area, $A=N_A\Omega_\nu$, and that the real part of the action is L times the real part of the action for motion along a single line segment, $\tilde{S}_0(L,N_A)=\alpha_0 L\pm i2\pi fN_A$. In fact, the action associated with a single ring exchange takes this form only for paths with a very high degree of symmetry, of which the

straight-line path shown in Fig. 3(a) and considered in the next section, is a particularly simple example. A general path has many corners near which the electron deviates from straight-line motion. As noted previously, this implies that the action is not simply $\tilde{S}_0$. We can express the effect of these deviations by considering the average contribution to Z from all exchange loops of fixed length L and fixed number of enclosed plaquettes N_A:

$$\langle e^{-\tilde{S}[R^c]}\tilde{D}[R^c]\rangle_{L,N_A}=(\cdots)e^{-\tilde{S}_0(L,N_A)}\int dS'dA'e^{-S'\pm i2\pi fA'/\Omega_\nu}P(S',A'\mid L,N_A)\ . \tag{2.24}$$

Here $A=N_A\Omega_\nu+A'$ is the enclosed area and $P(S',A'\mid L,N_A)dS'dA'$ is the probability that one of these rings chosen at random will have action $\tilde{S}=\tilde{S}_0(L,N_A)+S'\pm i2\pi fA'/\Omega_\nu$. We expect that in the limit of large L, S' and A' should be approximately independent Gaussian random variables with first moments δ_S and δ_A, and second moments Δ_S and Δ_A, respectively. Therefore, in this limit, the effect of deviations from a straight-line-segment path can be expressed as a simple renormalization of the exponent in Eq. (2.23):

$$\alpha L-i2\pi fN_A\rightarrow[\alpha+\delta_S/L-\Delta_S/2L+(2\pi f)^2\Delta_A/L]L\pm i2\pi f(N_A+\delta_A)\ . \tag{2.25}$$

We need to determine the L and N_A dependence of δ and Δ for this expression to be useful. If we assume that the dominant interactions which cause the path to deviate from a straight-line segment are determined by the local configuration of corners of the path, then P is approximately independent of N_A; δ_S, Δ_S, and Δ_A are proportional to L, and δ_A vanishes like $1/L$ for large L. (In fact, the discreteness of the lattice implies the presence of an order L^0 term in δ_A. We believe this term is an artifact of the crystalline lattice.) From Eq. (2.25), this implies that the net effect of corners on the contribution from large ring exchanges is to renormalize α to $\alpha+\alpha_1$. To obtain an approximate upper bound on the magnitude of α_1, we have compared the action of extreme case of a zigzag path, holding all nontunneling electrons fixed [see Fig. 3(b)] with that of the straight-line path discussed below. The resulting bound on α_1 is $\alpha_1\approx\alpha$. For the typical path in which the density of corners is much lower and relaxation effects are included, α_1 will be much smaller.

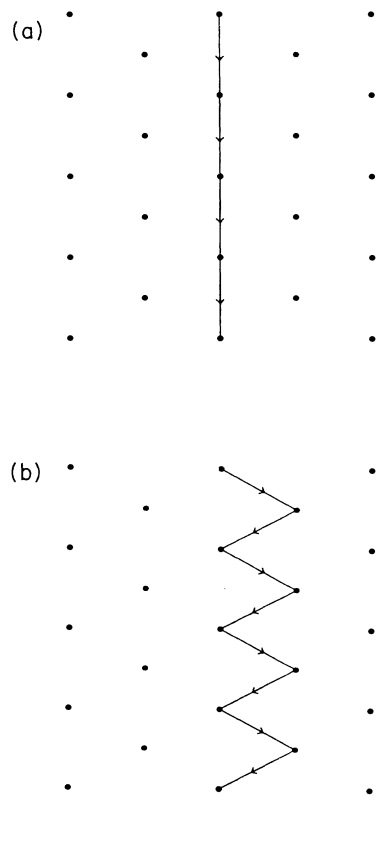

FIG. 3. (a) A "straight-line exchange" path. (b) Zigzag path.

D. Calculation of $\alpha(\nu)$

The numerical value of the tunneling coefficient $\alpha(\nu)$ determines whether cooperative ring exchanges contribute significantly to the partition function at a given density ν. We estimate this coefficient for a particularly simple exchange path. Consider the path in which one row of electrons exchanges one step in the x direction, so $X_j(\beta)=X_j(0)+a_\nu$ and $Y_j(\beta)=Y_j(0)$, where $a_\nu=(4\pi/\sqrt{3}\nu)^{1/2}$ is the lattice constant of the Wigner crystal. We impose periodic boundary conditions in the x direction, $X_j(\tau)=X_{j+L}(\tau)$. Since this path encloses no area, the action can be chosen to be pure real. To make the calculation tractable, we assume that only the electrons in this one row move, in the background of the static potential of all the other electrons. Thus we probably *overestimate* $\alpha(\nu)$.

The classical action, and hence $\alpha_0(\nu)$, can be readily calculated numerically (see Appendix D), but in order to calculate the fluctuation determinant and $\Delta\alpha(\nu)$ it is convenient to work with an analytic approximation for the actual potential in the action. We have checked numerically that for $|Y_j|\ll a_\nu$, the actual potential is well approximated by

$$V=\frac{e^2}{\epsilon a_\nu}\left\{\sum_{j=1}^{L}\left[\frac{Q_y}{2}\left[\frac{Y_j}{a_\nu}\right]^2+\frac{Q_x}{(2\pi)^2}[1-\cos(2\pi X_j/a_\nu)]\right]\right.$$
$$\left.+\sum_{\substack{k,j\\(k>j)}}\frac{1}{2}\left[K_x(k-j)\left[\frac{X_k-X_j}{a_\nu}\right]^2+K_y(k-j)\left[\frac{Y_k-Y_j}{a_\nu}\right]^2\right]\right\}. \tag{2.26}$$

For $\nu=\frac{1}{3}$, we found that the best fit to the actual potential was obtained with $Q_x=0.260$ and $Q_y=2.44$, and that $\mathbf{Q}$ and $\mathbf{K}(j)$ are only weakly dependent on ν. That $Q_x/Q_y=0.1067\ll 1$ reflects the important fact that when the entire row moves coherently in the z direction, each electron is moving toward a site left vacant by its neighbor, and so the potential barrier is very much less than for motion in the y direction.

With this form of the action, both the classical action and the fluctuation determinant can be evaluated explicitly. Since S is a quadratic form in Y_j, the motion in the y direction can be integrated out exactly. This yield a new, effective action S^{eff} for the x motion, with a quadratic kinetic energy

$$S^{\text{eff}}=\frac{e^2}{\epsilon}\int_0^\beta\frac{d\tau}{a_\nu}\left[\sum_{\substack{j,k\\(j>k)}}[\tfrac{1}{2}\dot\phi_j M(j-k)\dot\phi_k+2\pi^2K_x(j-k)(\phi_j-\phi_k)^2]+\sum_j Q_x(1-\cos\phi_j)\right], \tag{2.27}$$

where $\phi_j=2\pi X_j/a_\nu$, $M(i-j)=(2\pi)^2a_\nu^6W_{ij}^{-1}$, and W_{ij}^{-1} is the matrix inverse of

$$W_{ij}=\delta_{ij}\left[Q_y+\sum_k K_y(k)\right]-K_y(i-j). \tag{2.28}$$

[$M(i-j)$ is an exponentially decreasing function of $|i-j|$, and hence $M^*=\sum_j M(j)=(2\pi)^2a_\nu^6/Q_y$ acts as an effective mass.] S^{eff} is the action for a one-dimensional sine-Gordon chain. The classical path satisfying the boundary conditions, $\phi_j(0)=0$ and $\phi_j(\beta)=2\pi$, corresponds to the simultaneous coherent motion of all the electrons, i.e., $\phi_j(\tau)=\phi_0(\tau)$. Hence, $\tilde S[R^c]=\alpha_0(\nu)L$, where $\alpha_0(\nu)=(Q_x/Q_y)^{1/2}(8/\sqrt{3}\pi)\nu^{-1}$, is independent of $\mathbf{K}$. Note that, as promised, $\alpha_0(\nu)$ is rather small due to the softness of the potential in the x direction. The characteristic classical time over which the transition occurs can also be readily calculated and one finds $\tau_0(\nu)=a_\nu^2/(Q_xQ_y)^{1/2}(e^2/\epsilon l)^{-1}$.

To evaluate the fluctuation determinant $\tilde D[R^c]$ we approximate the discrete sine-Gordon chain in Eq. (2.27) by a field theory with a finite ultraviolet cutoff $\Lambda\sim 1/a_\nu$ and then use known results for the sine-Gordon field theory.[30] Of course the effects of fluctuations with wave number k of order Λ are treated very crudely in this approximation. However, if the quantum parameter $g/8\pi$ (defined below) is small compared to 1, the effect of short-wavelength fluctuations is small, as reflected in the weak Λ dependence of the results. Usually, to take a continuum limit of Eq. (2.27), $(\phi_j-\phi_k)$ is replaced by $(j-k)a_\nu\partial_x\phi$, but since $\sum_j j^2K_x(j)$ is log-divergent, this procedure does not work; the continuum model must be constructed with greater care. To do this, we examine the free propagator obtained from Eq. (2.27) by approximating the cosine by a quadratic potential, and relate it to the corresponding free propagator of the continuum model. The free propagator for the lattice model is

$$G_0(k,\omega)=\{M^*\omega^2+K_0(ka_\nu)^2[\ln(1/ka_\nu)+\tfrac{3}{2}]+Q_x\}^{-1},$$

while for a continuum theory with effective elastic constant K, the propagator is

$$\tilde G_0(k,\omega)=[M^*\omega^2+K(ka_\nu)^2+Q_x]^{-1}.$$

For Kk^2 smaller than Q_x, the propagator is approximately independent of k, while for large k the propagator is small. Thus, over the relevant range of k, the two propagators are approximately equal for

$$K=K_0[\tfrac{3}{2}-\ln(k_Qa_\nu)]\approx\tfrac{1}{2}K_0[\ln(K_0/Q_x)+3],$$

where $k_Qa_\nu=(K/Q_x)^{1/2}$. What emerges from this analysis is

$$S^{\text{eff}}\approx\frac{1}{g}\int_0^{\beta'}d\tau\int_0^L d\tau\left[\frac{\dot\phi^2}{2}+\frac{\phi_r^2}{2}+m_0^2[1-\cos\phi]\right], \tag{2.29}$$

where, by rescaling our units of time so that $\beta'=\beta/m_0\tau_0$, we are left with a single dimensionless classical coupling constant $m_0=(Q_x/\kappa)^{1/2}a_\nu^{-1}$ and a single quantum parameter

$$g/8\pi=(Q_y/\kappa)^{1/2}(\sqrt{3}/8)\nu\approx 0.24\nu, \tag{2.30}$$

where $G/8\pi=1$ marks the point at which the classical ground state becomes unstable. Note that for all relevant values of ν, we have that $g/8\pi\ll 1$.

From Eq. (2.16), the effect of Gaussian fluctuations can be readily calculated and the results can be summarized as follows. (1) They produce quantum renormalizations of the bare parameter m_0 which enters the action, which simply results in m_0 being replaced by $m=m_0(m_0/2\Lambda)^{g/8\pi}\sim m_0(Q_x/\kappa)^{g/16\pi}$. Physically, this reflects the fact that because of the zero-point fluctuations of the field, the effective barrier height between the different minima of the potential is less than its classical value. (2) They shift the soliton creation energy, measured in units of the renormalized frequency m, to

$E_s/m = 1 - g/8\pi$ due to the temporary reduction of the zero-point energy of the field that occurs during the tunneling event (a dynamic Casimir effect). (3) The zero mode produces a prefactor of the form $(\tau_0)^{-1} d\tau (\tilde{S})^{1/2}$. Combining all these results, we obtain at last the expression

$$\tilde{D} e^{-\tilde{S}} = (\tau_0)^{-1} d\tau \exp[-\alpha(\nu) L + O(\ln L)] , \tag{2.31}$$

where

$$\alpha(\nu) = \nu^{-1} \left[\frac{8}{\sqrt{3}\pi} \right] \left[\frac{Q_x}{Q_y} \right]^{1/2} \left[\frac{Q_x}{4\kappa} \right]^{g/16\pi} \left[1 - \frac{g}{8\pi} \right] , \tag{2.32}$$

and $g/8\pi \approx 0.24\nu$ is defined in Eq. (2.30). For $\nu = \frac{1}{3}$, $g/8\pi \approx 0.08 \ll 1$, and $\alpha(\frac{1}{3}) \approx 1.0$. The bare value α_0 is 1.48 at $\nu = \frac{1}{3}$, so the the quantum renormalization is $\sim 33\%$ at this density. The tunneling coefficient $\alpha(\nu)$ is calculated in Eq. (2.32) is shown in Fig. 6.

III. MAPPING ONTO A DISCRETE MODEL

A. Sum over paths

Having obtained an approximate expression for the action due to a single isolated ring, we now turn to the task of enumerating all such exchange rings and summing their contributions to the partition function. If $\alpha(\nu)$ is large, so that the system is in the sparse-ring phase, this can be done by making use of the dilute-gas approximation:

$$\ln Z \approx \sum_{L, N_A} 2\mathcal{N}(L, N_A) \left[\frac{\beta}{\tau_0} \right] (\cdots) e^{-\alpha L} \times \cos(2\pi f N_A) \langle e^{-\delta S} \rangle_{L, N_A} , \tag{3.1}$$

where $\mathcal{N}(L, N_A)$ is the number of polygons which can be drawn on a triangular lattice with circumference of length L and with N_A enclosed plaquettes. The factor $(\beta/\tau_0)(\cdots)$ comes, as in Eq. (2.22), from the fluctuation determinant, the factor $2\cos(2\pi f N_A)$, where $f = \frac{1}{2}(\nu^{-1} - 1)$, results from the interference between paths in which the exchange occurs in the clockwise and counterclockwise directions, and the term $\langle e^{-\delta S} \rangle_{L, N_A}$ is the average over all shape-dependent variations in the classical action for paths of fixed L and N_A. For large L, $\mathcal{N}(L, N_A) \sim \mathcal{K}^L$, where $\mathcal{K} \sim 4$ is the connectivity of the lattice. It is clear from Eq. (3.1) that the dilute-gas approximation is valid only if $\alpha \gg \ln \mathcal{K}$. For $\alpha < \ln \mathcal{K}$, the entropy associated with large paths outweighs the "energy" αL. However, in the dense-ring (small-α) phase the dilute-gas approximation breaks down, as signalled by the observation that the free energy computed from Eq. (3.1) is superextensive.

For small α, the sum over the important classical paths becomes considerably more complicated. Firstly, the important paths consist of overlapping and intersecting rings of electrons exchanging essentially simultaneously so that the action associated with such a path is not simply the sum of the actions associated with the constituent rings. We will refer to this as interactions between rings. Secondly, we can no longer restrict our attention to rings in which the electrons move only to nearest-neighbor sites; for small α, exchanges involving further neighbors also become important.

We have not been able to develop a well-controlled approximation for summing the contributions of all these paths. We have, however, developed an approximate method for summing the contribution of an important subclass of these paths by relating the sum to the partition function of a two-dimensional classical spin model. The equivalence to the spin model is asymptotically correct for large α, and we believe it captures the essential features of the dense-ring phase which occurs at small α. Since the mapping is not exact, we begin with a general discussion of the essential ingredients. (1) We consider the subclass of classical paths which can be constructed as a linear superposition of individual ring-exchange events. Each individual event is characterized by a set of directed segments along the nearest-neighbor bonds which comprise the ring and which specify the direction of the exchange motion, and by an imaginary time which specifies when the exchange event occurs. (2) The real part of the action increases approximately linearly with the net length of the exchange rings. (3) The imaginary part of the action is proportional to the directed area enclosed by the exchange paths, due to the Aharonov-Bohm effect. In addition, we associate an extra contribution to the imaginary part of the action, also proportional to the enclosed area, which incorporates the Fermi statistics. (4) The exchange motion occurs on a characteristic (imaginary) time scale of order τ_0. Exchange events that occur at times much greater than τ_0 apart are essentially noninteracting.

With these points in mind, we construct our spin model in three steps. First, we divide the time interval β into time slices of approximate duration τ_0. All exchanges that occur in different time slices are assumed to be independent and noninteracting. Thus, $Z \simeq (Z_{\text{slice}})^{\beta/\tau_0}$, where Z_{slice} is the sum over all exchanges that occur in a given time slice. This approximation is plausible since the exchange paths are exponentially localized in time.

Within a given time slice, we associate with each exchange path a set of integer valued "spins" S_λ defined on the (dual) lattice of plaquetts such that S_λ is equal to the number of clockwise exchange loops *minus* the number of counterclockwise exchange loops that encircle plaquette λ (see Fig. 4). Thus the classical paths are the domain walls of the spin model. To each classical path there corresponds a unique spin configuration on the dual lattice. However, in the presence of overlapping or intersecting loops, the mapping is not one to one; more than one classical path may correspond to each spin configuration. For example, when two intersecting ring exchanges occur in the same time slice, we obtain spin configuration of the sort shown in Fig. 5(a). This spin configuration corresponds to at least two possible exchange paths, depending on whether the ring to the left or the ring to the right exchanges first. There are also paths which overlap on a line segment, as shown in Figs. 5(b) and 5(c). If the com-

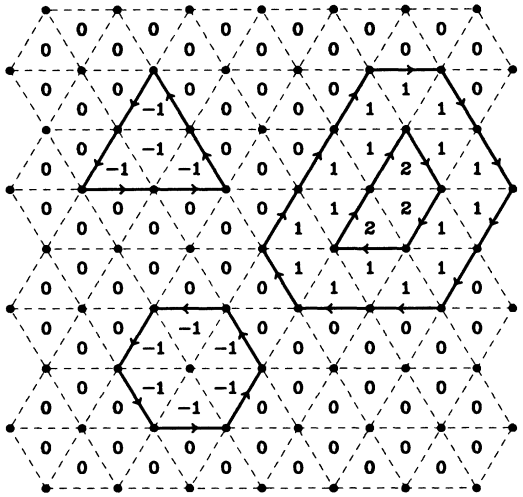

FIG. 4. Mapping to a spin model: The integer spin variables assigned to a plaquette reflects the net ring-exchange circulation about that plaquette in a given time slice.

mon segment is traversed in the same direction by both paths, as in Fig. 5(b), again there is a degeneracy in the mapping since either the path on the right or the path on the left can exchange first. However, the degeneracy is much more important in the case where the common segment is traversed in opposite directions, as in Fig. 5(c). The resulting spin configuration is the same as if the common segment were not traversed at all. This is not likely to be important since we expect the action associated with the path in which the segment is multiply traversed to be considerably larger than the action associated with the path in which the segment is not traversed at all. Indeed, we have found that if we suppress the contribution of paths in which any segment is multiply traversed during a given time step it does not change our results qualitatively (see below).

We now have an approximate representation of the sum over classical paths in terms of a sum over classical spin configurations. The remaining step is to construct a spin Hamiltonian such that the "energy" associated with a given spin configuration is equal to the action associated with the corresponding classical path. This can be done to arbitrary levels of complexity, but in light of the fact that the mapping onto the spin model is itself only approximate, we have contented ourselves with studying the simplest model which is consistent with the general features of the classical paths listed above. Thus, we associate with each spin configuration an energy

$$H_{\mathrm{DG}}=\alpha \sum_{(\lambda,\gamma)} (S_\lambda - S_\gamma)^2 + 2\pi i \sum_\lambda f_\lambda S_\lambda \ , \tag{3.2}$$

where $\langle \lambda,\gamma \rangle$ denotes a nearest-neighbor pair on the dual lattice, $f_\lambda = \Phi_\lambda/\Phi_0 - \frac{1}{2} = (\nu^{-1}-1)/2$, and $\Phi_\lambda/\Phi_0 = \frac{1}{2}\nu^{-1}$ is the magnetic flux through plaquette λ in units of the Dirac flux quantum. H_{DG} can be recognized as the Hamiltonian of the discrete Gaussian (DG) model in an imaginary field.[31] The sum over paths within a given time slice can thus be approximated by

$$Z_{\mathrm{slice}} \simeq Z_{\mathrm{DG}} \equiv \mathrm{Tr}\, e^{-H_{\mathrm{DG}}} \ . \tag{3.3}$$

The mapping to the discrete Gaussian model makes the following assumptions concerning the action of various classical paths.

(1) There are various interactions between paths which reflect the fact that multiple classical paths correspond to each spin configuration.

(2) There is an effective interaction between loops which share one or more traversed segments in that any segment traversed n times carries with it an action $n^2\alpha(\nu)$.

(3) There are no interactions associated with corners or bends in the exchange path; the real part of the action is simply proportional to the length of the path.

(4) There are no interactions between disjoint exchange loops.

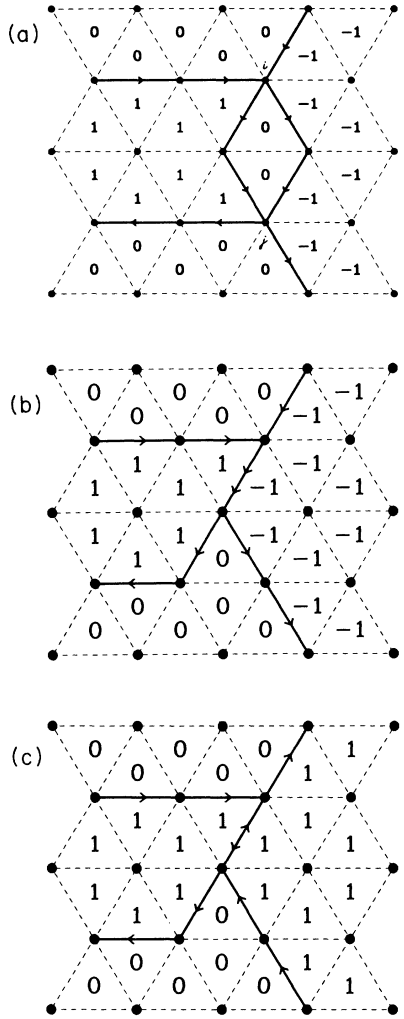

FIG. 5. Unfaithful aspects of the mapping. (a) A spin configuration which corresponds to two intersecting exchange paths. (b) A spin configuration corresponding to two exchange paths which overlap additively on a single segment. (c) A spin configuration corresponding to exchange paths which overlap in a canceling sense on a single segment.

Assumption (1) concerns the fact that the mapping is not one to one as has already been discussed. The most important example of this is that paths in which a given segment is traversed in opposite directions is not included at all in Eq. (3.3); it is as if there were an infinite action associated with such paths. On the other hand, if the segment is traversed more than once in the *same* direction, a finite action is associated with the path, as stated in assumption (2). In the absence of loop-loop interactions, the action associated with an n-times–traversed segment, such as the $n=2$ exchange shown in Fig. 5(b), would be $n\alpha$, whereas in the DG model it is $n^2\alpha$. We choose an interaction of the form $(S_\lambda - S_\gamma)^2$ since the tunneling amplitude in a magnetic field is proportional to the *square* of the distance trasversed. However, we note that the solid-on-solid model,[32] with an interaction of the form $|S_\lambda - S_\lambda|$, is believed to lie within the same universality class as the discrete Gaussian model. If we had represented the sum over paths with a solid-on-solid model we would have neglected interactions between overlapping loops (other than those included from mapping different exchange paths onto a single spin configuration). This fact suggests an insensitivity of the results of our analysis to the actual approximation used for loop-loop interactions. In fact, one could restrict neighboring spin variables to differ by 0 and ± 1 only, thereby eliminating all configurations which correspond to loops that share segments, and still obtain similar results. This case is a special solid-on-solid model which has transition temperature very close to that for the DG model.[33]

Assumption (3) says that for paths with only singly traversed segments, the real part of the action is assumed to be simply αL, independent of the shape of the exchange path, i.e., how many corners it has, or how many intersections it has (although some interaction effects due to intersections are included as discussed above.) These approximations could, in principle, be improved by including further-neighbor and multispin interactions in the Hamiltonian, i.e., an interaction which counted the number of corners or the number of intersections. However, we do not expect the inclusion of short-ranged spin interactions to change the nature of the model in any essential manner. Interactions between spatially separated segments of the exchange path are not zero [assumption (4)], but they appear to be sufficiently short ranged that they do not have any important qualitative effects. For instance, if we consider two simultaneously exchanging rings of N electrons, each separated by a distance X which is large compared to their radii, we can calculate the interaction energy using a multipole expansion. The lowest-order contribution comes from the $l=N$ multipole and the interaction energy falls off as $r_0(r_0/X)^{2N+1}$, which is small in comparison with the local line energy of the ring. When rings are in close proximity, where the multipole expansion converges poorly, the interaction effects are potentially important. Although we have no proof that such short-ranged interactions are not qualitatively important, we believe that such terms may also be introduced as additional short-ranged spin-spin interactions in the DG Hamiltonian which do not alter the nature of the transition.

We have discussed the steps which lead from the sum over classical paths to the discrete Gaussian model, highlighting the approximations that arise at each step. While it is possible to refine the process by introducing additional interactions in the spin model, there are inherent errors associated with the time-slice approximation. Thus the spin model is not reliable on a quantitative level. The value of α which appears in the DG model, for example, should be interpreted as an effective α, which is only roughly related to the value of α appropriate for the motion of a single isolated ring which was calculated in the previous section. However, we also believe that the relation between the sum over classical paths and a spin model with similar long-distance behavior to the discrete Gaussian model is correct despite our inability to establish an exact correspondence. This belief is based on the fact that the discrete Gaussian model incorporates all the features of the sum over classical paths, listed at the beginning of this section, which we believe embody the essential physics of the problem.

B. Equivalence with other models

The discrete Gaussian Hamiltonian is related to other well-studied models. For example, application of the Poisson summation formula produces an *exact* equivalence to the spin-wave–vortex-gas system. In addition, the DG model may be mapped onto the planar (XY) model using a duality transformation and the Villain approximation. (In the presence of an imaginary field, the DG model maps onto the *frustrated* XY model.) All these models have received a great deal of attention, both analytical and numerical, and many existing results may be applied directly to our ring-exchange model. In Appendix E we review the equivalence between the DG model of Eq. (3.2), the frustrated XY model, which is described by the Hamiltonian

$$H=\frac{1}{2\alpha}\sum_{\langle \mathbf{r},\mathbf{r}'\rangle}[1-\cos(\theta_r-\theta_{r'}-A_{rr'})]\ , \tag{3.4}$$

and the vortex-gas model

$$H_{\mathrm{VG}}=-\frac{\pi}{2\alpha}\sum_{i,j}{}'(m_i-f_i)G_{ij}(m_j-f_i)\ . \tag{3.5}$$

In Eq. (3.4) the dynamical variables are the angles $\{\theta_r\}$ and the sum is over all nearest-neighbor pairs $\langle \mathbf{r},\mathbf{r}'\rangle$ on the triangular lattice $\mathcal{L}$. This model has been used to describe Josephson-junction arrays in a transverse magnetic field,[34] where superconducting islands interact via a proximity coupling. The vector potential $A_{rr'}$ lives on the links of $\mathcal{L}$ and is constrained by the requirement that the integral $\oint \mathbf{A}\cdot d\mathbf{l}$ around a plaquette yield the total magnetic flux through that plaquette, which we write as $2\pi f_k$ in units of the elementary flux quanta: $\sum_{\text{plaquette}} A_{rr'}=2\pi f_k$, with $A_{rr'}\equiv(2e/\hbar c)\int_r^{r'}\mathbf{A}\cdot d\mathbf{l}$. In Eq. (3.5) the dynamical variables are the integer charges m_i and the prime on the sum denotes that only neutral configurations contribute to the partition function, i.e., the constraint $\sum_i (m_i-f_i)=0$ is imposed. The asymptotic form of the lattice Green's function for large $|i-j|$ is $\mathcal{G}_{ij}\sim\ln|i-j|$. Note that in

these models, since local integral flux increments are "invisible" (i.e., the system is invariant under $f_k \rightarrow f_k + 1$), all thermodynamic properties are dependent only on the fractional part of f_k. If the flux is uniform (i.e., $f_k = f \ \forall k$), an additional invariance, $f \rightarrow -f$, results.

C. Critical couplings and commensuration

In our model, the coupling α and the flux per plaquette f are not independent. Rather, they both depend on the dimensionless density ν, with $f(\nu) = (1+\nu)/2\nu$ and $\alpha(\nu)$ derived earlier. In investigating our one-parameter phase diagram, however, we shall find it useful to consider α and f as independent parameters.

There have been several approaches to the statistical mechanics of models such as those defined in Eqs. (3.4) and (3.5), including mean-field theory,[35] Monte Carlo,[34,36,37] and ansatz ground states.[38] All these studies indicate that the ordered-state properties are very sensitive to the value of f. In general, the critical coupling α_c is an increasing function of the "degree of rationality" of f. In other words, writing $\mathcal{R}(f) = p/q$, with p and q relatively prime, one finds that α_c is largest when the denominator q is smallest. The value of f which leads to the greatest α_c is $f=0$, i.e., $\nu = 1/(2j+1)$. Since for $f=0$ all rings add in phase it follows that, independent of f, the 2D electron gas (2DEG) is in the sparse ring phase whenever $\alpha(\nu)$ is larger than α_c at $f=0$.

Since α_c is a nonuniversal quantity, one can only obtain an estimate of its value from calculations for the various spin models considered above. On the square lattice, for example, estimates of the transition temperatures give a range of α_c from 0.45 to 0.87, where the lower values come from the XY model[39] and the higher values come from the DG or solid-on-solid models.[33] The values of α_c are larger for the lattices of interest (namely, the honeycomb lattice for the DG model and the triangular lattice for the XY model) and range between 0.7 and 1.3.[40] These differences depend on the details of the models (i.e., the short-distance behavior). Since the mapping to the spin model is not exact, there is no compelling reason to chose any particular one of these values of α_c. However, favoring (somewhat arbitrarily) the DG model, since this was our starting point, we use the estimate of $\alpha_c \approx 1.1$ at $f=0$ for illustrative purposes.

A comparison of our calculated function $\alpha(\nu)$ and the corresponding critical coupling $\alpha_c(\nu)$ is shown in Fig. 6. At low densities $\alpha > \alpha_c$, and the system is in the sparse-ring phase. (In the language of the vortex gas, this is the screening phase.) As the density is increased, the curve $\alpha(\nu)$ dips below $\alpha_c(\nu)$, provided that $f(\nu)$ attains a simple rational value, and a dense-ring phase results. Though the function $\alpha_c(\nu)$ exhibits a local cusps at fillings other than $\nu_j = 1/(2j+1)$, these higher-order commensurations are probably irrelevant to the fractional quantized Hall effect, as the figure suggests. Using the approximations for α and α_c discussed above, the only lowest-order commensurate Hall state that our theory allows is the $\frac{1}{3}$ state. Hierarchical generalizations of the cooperative ring-exchange theory will be discussed in the following section.

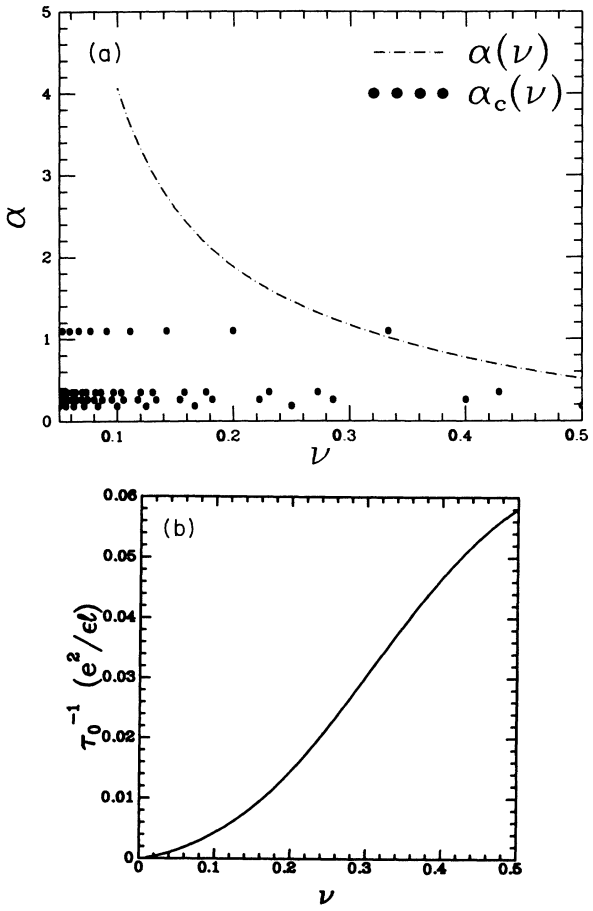

FIG. 6. (a) A comparison of the calculated values of $\alpha(\nu)$ to the estimated critical coupling $\alpha_c(\nu)$ (see discussion in text). The Maki-Zotos value, $\alpha_{MZ}(\nu) = \pi/(\nu\sqrt{3})$ is much larger than $\alpha(\nu)$. For $\nu = \frac{1}{3}$, $\alpha_{MZ} \approx 5.2$. (b) Unrenormalized value of the inverse tunneling time τ_0^{-1} vs filling factor fraction ν.

D. Deviations from perfect commensuration

The most straightforward way in which a state might change its density but still retain energy-favoring correlations is via uniform dilation. A central feature of the Laughlin theory is the incompressibility of the ground state, which disallows any such infinite-wavelength charged excitations. This is in great contrast to the normal concept of a crystal, which can dilate, thereby changing its density at very little energy cost.

A uniform dilation in our model is described by changing the filling fraction ν. It is then natural to ask how the free energy of the system depends on the deviation $\delta\nu$, with $\nu = \nu_j + \delta\nu$. For $\delta\nu$ small, we can take $f = -\delta\nu/2\nu_j^2$, and the allowed vortex strengths will be integers minus $f(|f| \ll 1)$. Without loss of generality, we consider the case $f > 0$, i.e., uniform expansion. The chemical potential for a single vortex of (integer) strength q is $\mu_q = \pi^2 q^2/3\alpha$, which strongly discourages excess vorticity. The system also must satisfy the constraint of overall charge neutrality. These conditions require that for small α, the ground state consists of a superlattice of vortices of

strength $1-f$ atop a uniform $q=-f$ state, the superlattice constant being determined by the neutrality constraint.[38] This leads to an energy per plaquette of $\mathcal{E}\simeq(\pi/8\alpha)f\ln(1/f)$. Allowing for arbitrary sign of f, one finds

$$\mathcal{E}\simeq-\frac{\pi}{8\alpha}|f|\ln|f|\ , \tag{3.6}$$

and the ground-state energy per plaquette has a *cusp* at $f=0$. Of course, what we really need is the free energy per plaquette, $\mathcal{F}$ at temperature $k_BT=1$. By considering thermal excitations in the vortex gas, we obtain

$$\mathcal{F}\approx\frac{-\pi}{8\alpha\epsilon_{VG}}|f|\ln|f|\ , \tag{3.7}$$

where ϵ_{VG} is the dielectric function of the vortex gas. The physical origin of the cusp in $\mathcal{F}$ is clear. At slightly incommensurate densities, different rings within the same time slice lose their phase coherence. This decreases the total partition sum, thus increasing the free energy. In the sparse-ring phase, the increase $\delta\mathcal{F}$ is analytic. However, in the dense-ring phase, the exchange condensate induces a rigidity with respect to uniform dilations, as reflected by the cusp in Eq. (3.7).

IV. ELEMENTARY EXCITATIONS

A. Quasiparticles

The fact that $d^2\mathcal{E}/d\nu^2$ is negative for ν near ν_j leads us to consider an inhomogeneous ground state at $\nu_j+\delta\nu$ in which local distortions (analogous to Laughin's quasiparticles) account for the deficit or surplus density. In the dense exchange regime, rings which enclose the distortion will acquire an additional Aharonov-Bohm phase $\Delta\theta=2\pi B\delta A/\phi_0$ relative to those rings that do not. Thus, the creation energy of such a defect would be logarithmically infinite unless the Aharonov-Bohm phase is an integer multiple of 2π, that is $\delta f=\delta A/2\pi l^2$ is an integer, or equivalently, the quasiparticle charge is *quantized* in units of $e^*=\nu e$. The quasiparticle creation energy is a sum of a term due to the real $(1/r)$ Coulomb force, which is a decreasing function of the quasiparticle radius, R_{qp}, and a ring-exchange term which is an increasing function of R_{qp}.

To calculate the equilibrium quasiparticle radius and energy, R_{qp} and E_{qp}, we consider a trial quasiparticle state in which the area distortion δA is equally shared by a number of plaquettes comprising a roughly circular region in the Wigner lattice. We assume that the quasiparticle is a charge ν disturbance atop a primitive $\nu=1/m$ ground state, in which case the ground-state configuration of the associated vortex-gas system consists of a single vortex $m_0=1$ surrounded by $N=\pi R^2/\Omega_\nu$ "expanded" plaquettes of area $\Omega_\nu+\delta\Omega$ and vorticity $\delta f=1/N$. We treat the quasiparticle as a two-dimensional one component plasma,[41] in which the vortex corresponds to an electron, and the expanded plaquettes to the neutralizing background. This assumes that the quasiparticle extends over a reasonably large number of plaquettes, although the conclusions are nonetheless qualitatively valid even in the small-quasiparticle limit. The excess ring-exchange energy of this configuration is then

$$\begin{aligned}E_r&=\frac{\pi}{\alpha\tau_0}\sum_k \mathbb{1}\cdot G_{0k}\delta f_k-\frac{\pi}{\alpha\tau_0}\sum_{\substack{j,k\\(j<k)}}\delta f_j G_{jk}\delta f_k\\&\simeq\frac{\sqrt{3}\pi}{2\alpha\tau_0}\left[\ln\left[\frac{R}{a_\nu}\right]-\frac{3}{4}-\frac{\pi}{\sqrt{3}}\right]\ ,\end{aligned} \tag{4.1}$$

where we have used the long-distance behavior of the honeycomb-lattice Green's function,

$$\lim_{R_{ij}\to\infty}\mathrm{Tr}G_{ij}\simeq\sqrt{3}\ln(R_{ij}/a_\nu)+\pi\ , \tag{4.2}$$

derived in Appendix F. The approximate Coulomb energy of the distortion is given by

$$E_C=\frac{J\nu^2e^2}{\epsilon R}\ , \tag{4.3}$$

where J is a constant, given by

$$J=\frac{1}{2\pi}\int^1 d^2x\int^1 d^2x'\frac{1}{|x-x'|}\ , \tag{4.4}$$

which can be modified to properly account for lattice-corrugation effects. Balancing these two energies by setting $d(E_r+E_C)/dR=0$, we find

$$\begin{aligned}R_{qp}&=\frac{2J}{\sqrt{3}\pi}\frac{e^2}{\epsilon l}(\nu^2\alpha\tau_0)l\ ,\\E_{qp}&=\frac{\sqrt{3}\pi}{2\alpha\tau_0}\left[\ln\left[\frac{R_{qp}}{a_\nu}\right]+\frac{1}{4}-\frac{\pi}{\sqrt{3}}\right]\ .\end{aligned} \tag{4.5}$$

As a function of ν, $R_{qp}(\nu)$ is monotonically decreasing, which reflects one's intuition that a dense exchange gas prefers a small quasiparticle radius, the logarithmic ring-exchange energy overwhelming the lattice Coulomb energy in this limit. For large quasiparticles, the effective potential, $v(\mathbf{r})=-\pi G(\mathbf{r})/\alpha\tau_0$, should be screened by the vortex-gas dielectric function, e.g., $v(\mathbf{r})\to v(\mathbf{r})/\epsilon(\mathbf{r})$. As one enters into the sparse-ring regime, virtual vortex-antivortex excitations completely screen out the strong logarithmic interaction, rendering the potential effectively short ranged. It is known that the large distance limit of $\epsilon(\mathbf{r})$ has an *infinite* discontinuity at the Kosterlitz-Thouless transition point, and that $\epsilon^{-1}(\mathbf{r}\to\infty)$ is zero in the sparse-ring regime.[42] Our theory therefore predicts an abrupt vanishing of the charged excitation gap at the transition point. [To be precise, the gap vanishes abruptly as $\alpha(\nu)$ increase above α_c *with* $f=(\nu^{-1}-1)/2$ *held fixed.* This may hold some relation to the apparent first-order transition seen by Haldane and Rezayi[15] when the pseudopotential components of the interaction potential are varied at fixed filling.]

B. Collective modes

While Laughlin's ground-state and fractionally charged elementary excitations provided the first microscopic picture of the fractional quantized Hall effect, a detailed understanding of the neutral collective mode was not avail-

able until the work of Girvin, MacDonald, and Platzman (GMP),[18] who generalized the Bijl-Feynman "single-mode approximation,"[43] originally used in deducing the phonon-roton curve for ^{4}He. GMP found that a liquid ground state, such as Laughlin's, would evidence a $k \to 0$ gap in the collective mode spectrum as a *generic* occurrence. Their magnetophonon-magnetoroton spectrum is also in excellent agreement with the numerical results of Haldane and Rezayi.[15,16] Our state, on the other hand, *seems* to share a certain kinship with the Wigner crystal, which has gapless magnetophonon excitations and a long-wavelength dispersion resembling $\omega_k \sim k^{3/2}$. These two pictures appear to be quite different, and a detailed investigation of the collective mode within the ring exchange theory is therefore required. Unfortunately, we have made only limited progress in this direction. The results are somewhat heartening, but there remain several major unanswered questions.

One possible scheme for investigating this issue is to adopt a lattice viewpoint and then work out the renormalized phonon frequencies in the presence of ring exchange. The basic idea is this: long-wavelength phonons oscillate on time scales $\omega^{-1} \gg \tau_0$, so by inverse adiabatically treating the coupled ring-phonon problem, one can trace out over the fast degrees of freedom (the ring exchanges) and arrive at an effective action for the phonons. The simplest such ring-phonon interaction would account for the phase variation incurred by rings which enclose deformed plaquettes. The ring exchange thus couples to the surplus and/or deficit magnetic flux:

$$H_{r\text{-ph}} = 2\pi i \sum_j S_j \left[\frac{\delta\phi_j}{\phi_0} \right] , \tag{4.6}$$

where $\delta\phi_j = B\delta A_j = \phi_0 \delta A_j / 2\pi l^2$, and δA_j is the change in area of plaquette j in the presence of the phonon field. We neglect corrections to the real part of the ring action due to the electron displacements, as we suspect that such contributions will be both small and smooth. We have also ignored terms proportional to the rate of change of $\delta\phi_i (\delta\dot{\phi}_i)$ although they may be important even in the adiabatic limit. We think $H_{r\text{-ph}}$ in Eq. (4.6) is the dominant term, since it is the phase commensuration, reflected by the $-|\delta f| \ln |\delta f|$ cusp in the free energy of the vortex gas, that should discourage long-wavelength density fluctuations and thus raise the frequency of the longitudinal branch of the phonon spectrum. (Actually, in the presence of a strong magnetic field, the low-lying collective mode is a longitudinal-transverse hybrid. This will prove to be of considerable importance below.)

The effective phonon Hamiltonian is obtained from

$$e^{-\tau_0 H_{\text{eff}}} = \operatorname*{Tr}_{\text{rings}} e^{-H_r - H_{r\text{-ph}}} . \tag{4.7}$$

Using the equivalence of the discrete Gaussian and spin-wave–vortex-gas models, we obtain

$$H_{\text{eff}} = -\tau_0^{-1} \ln \operatorname*{Tr}_{\{m_k\}} \exp \left[\frac{\pi}{2\alpha} \sum_{j,k} (m_j - f_j) G_{jk} (m_k - f_k) \right] , \tag{4.8}$$

with

$$f_j = f + \delta f_j = \tfrac{1}{2}(\nu^{-1} - 1) + \frac{\delta A_j}{2\pi l^2} . \tag{4.9}$$

(We have ignored the f_j independent term arising from the spin-wave component of the free energy.) One can now expand Eq. (4.8) in terms of the correlation functions of the vortex gas and obtain

$$H_{\text{eff}} = -\tau_0^{-1} \frac{\pi}{2\alpha} \sum_{j,k} \delta f_j \left[G_{j,k} + \frac{\pi}{\alpha} \sum_{l,l'} G_{jl} Q_{ll'} G_{l'k} \right] \delta f_k + O(\delta f^3) ,$$
$$Q_{jk} \equiv \langle (m_j - f)(m_k - f) \rangle_{\delta f = 0} . \tag{4.10}$$

Consider for the moment deviations about the odd denominator states, for which f can be taken to be zero. In this case, the vorticity-vorticity correlation $\langle m(\mathbf{R}) m(\mathbf{0}) \rangle$ behaves as $-R^{-\pi/\tilde{\alpha}}$ in the dense ring phase, where $\tilde{\alpha}$ is the bare coupling α renormalized by fluctuations of the vortex gas.[44] For our purposes it will be enough to take $\tilde{\alpha} \simeq \alpha$, in which case the Fourier space version of Eq. (4.10) becomes

$$H_{\text{eff}} = \tau_0^{-1} \frac{\pi^2}{\alpha} \sum_{\mathbf{k}} \delta f(\mathbf{k}) \left[\mathcal{G}(\mathbf{k}) - \frac{2\pi^2}{\alpha} \mathcal{G}(\mathbf{k}) Q(\mathbf{k}) \mathcal{G}(\mathbf{k}) \right] \times \delta f(-\mathbf{k}) + O(\delta f^3) ,$$
$$Q(\mathbf{k}) \simeq -Q_0 k^{(2-\pi/a)} \tag{4.11}$$

with $\mathcal{G}(\mathbf{k})$ the $\mathbf{k}$-space lattice Green's function discussed earlier. Provided $\alpha < \pi/4$, which is the Kosterlitz-Thouless criterion for being in the insulating phase of the vortex gas,[42] the long-wavelength density fluctuations interact via a k^{-2} coupling, and the plaquette distortions couple by a logarithmic interaction in real space. In the $\alpha > \pi/4$ region, the real-space interaction is short ranged. (When α is large, it is more convenient to expand the effective Hamiltonian in terms of the correlation functions of the discrete Gaussian model.)

The consequences of these results are most easily worked out within the framework of a continuum elastic theory (a detailed calculation is given in Appendix F) of a charged membrane in a magnetic field. The Lagrangian then contains four terms: kinetic, electromagnetic, local elastic, and "long ranged." In the absence of a field, the longitudinal and transverse modes have long-wavelength dispersions of the form

$$\omega_l^2(\mathbf{k}) = [v(\mathbf{k}) + C_1] k^2 ,$$
$$\omega_t^2(\mathbf{k}) = C_2 k^2 , \tag{4.12}$$

where $v(\mathbf{k})$ is the Fourier component of the long-ranged density-density interaction, and C_1 and C_2 are elastic constants. As alluded to above, the magnetic field strongly mixes these branches, and in the high-field limit one obtains a cyclotron mode with $\omega_+(k=0) = \omega_c$ [assuming that $\lim_{k \to 0} k^4 v(\mathbf{k}) = 0$], and a low-lying "magnetopho-

non" branch with

$$\omega_-(\mathbf{k})=\omega_l(\mathbf{k})\omega_t(\mathbf{k})/\omega_c \ . \tag{4.13}$$

In a two-dimensional system with $1/r$ interactions, $v(\mathbf{k})=2\pi e^2/k$, whence $\omega_l(\mathbf{k})\propto k^{1/2}$ and $\omega_t(\mathbf{k})\propto k$. This leads to the well-known result for the conventional 2D Wigner crystal[8,45] of $\omega_-(\mathbf{k})\propto k^{3/2}$.

In our model, the presence of a dense exchange gas leads to a logarithmic contribution to $v(\mathbf{r})$, which raises the longitudinal branch, giving $\omega_l(\mathbf{k})\propto k^0$. The transverse branch is of course unaffected by such an interaction, so the hybrid mode ω_- acquires a *linear* dispersion and only partially reflects the stiffness induced by the logarithmic interaction.

The existence of a $k=0$ gap in the magnetophonon spectrum, as predicted by Girvin *et al.*,[18] is so well confirmed by numerical simulations that one must conclude that an acoustic spectrum is the result of some faulty reasoning. We feel that there is no essential problem with the physics behind the ring-phonon Hamiltonian of Eq. (4.6), nor with the adiabatic approximation of Eq. (4.7). However, the expansion of $H_{\rm eff}$ in terms of the vortex-gas correlation functions is really a perturbation expansion in the δf_j. The effective Hamiltonian $H_{\rm eff}[\{\delta f_j\}]$ is manifestly invariant under the local gauge transformation $\delta f_j\rightarrow\delta f_j+1$, and this symmetry is clearly lost if one works to any finite order in perturbation theory. One expects that the vortex gas will respond (over *any* length scale) to an area deformation of magnitude larger than $2\pi l^2$ by nucleating a vortex charge, and this physics is obscured in the present treatment. The fully nonlinear model is extremely complicated, and we have not yet succeeded in determining what long-wavelength spectrum it reproduces.

C. Hierarchy schemes

The fractionally charged Coulomb gas has especially stable ground states at all rational values of f, as can be seen from Fig. 6, with the state at integer f being particularly stable This leads to the possibility of stable incompressible ground states in our original system (the 2DEG in a magnetic field) at various rational densities, with ν^{-1} odd being the most likely candidates for special stability. In fact, from our estimation of the tunneling coefficient $\alpha(\nu)$, it appears that $\nu=\frac{1}{3}$ may be the only stable incompressible state. However, the experimental observation of the FQHE at other rational densities[46] leads one to consider other possible CRE-stabilized ground states within our formalism. In this section we will consider two possible scenarios for stabilizing higher commensurability states. [Density $\nu=n/(2m+n)$ corresponds to $f=m/n$ or commensurability n.] The first is to consider as our starting configuration a distorted version of the original triangular Wigner crystal (WC) with unequal size plaquettes and hence a larger unit cell. The second is a hierarchy scheme, analogous to that considered previously on the basis of Laughlin's formalism, which constructs the higher-order commensurate states as condensates of a dense gas of the quasiparticles discussed in Sec. IV A. Let us begin by considering the first scenario.

The reason the state with integer $f=m$ is so stable is that it is wholly unfrustrated; the ground state has zero vorticity in each plaquette. This reflects that fact that for $\nu=(2m+1)^{-1}$ all rings add in phase. At all other densities the system is frustrated; each plaquette must have nonzero vorticity. For rational $f=m/n$, supercells can be defined consisting of n plaquettes which have zero net vorticity. This reflects the fact that certain classes of rings add in phase. However, the resulting stabilization energy is a subtle interference effect which would be small even for arbitrarily small α.

By distorting the lattice the frustration can be relieved so that all the rings add in phase, even at densities other than $\nu=(2m+1)^{-1}$, but at a cost in elastic (Coulomb) energy. We have discussed this competition in the context of the quasiparticle, and similar considerations hold here. If we consider the limit where the exchange energy dominates, then at any density other than $\nu=(2m+1)^{-1}$, the system distorts to form a mixture of large and small plaquettes, each with a half-integer flux penetrating it, so that the system is again unfrustrated. Even if we do not consider this extreme limit, it is clear that for $n>1$, the underlying triangular lattice will distort, since by increasing the size of the WC unit cell the system can reduce its frustration and hence lower its energy significantly. This effect is more important for larger n.

Let us consider the effect of lattice distortion on the stability of the high-order commensurate phases. Consider, for example, large n and $f_j=f\ll 1$. Then the ground state of the vortex gas consists of superlattice of vortices of strength $1-f$ atop a uniform $q=-f$ state, as described in Sec. III. If the lattice is distorted so that the area of each positively charged $(1-f)$ plaquette is reduced by an amount $\delta\Omega$ $[f_j=f-(1/2\nu)(\delta\Omega/\Omega_\nu)]$, then the charge on the positive sites will be reduced to $1-f-1/2\nu(\delta\Omega/\Omega_\nu)$. Since we consider only total-area preserving distortions, the charge on the negative sites is similarly reduced. Thus there is a reduction in the energy of the vortex gas (exchange energy) which is linear in $\delta\Omega$. Of course, since the perfect triangular lattice minimizes the electrostatic energy of the system, there is an increase in the direct energy, but this is quadratic in $\delta\Omega$. For general n, if $\delta\Omega$ is the magnitude of the lattice distortion, we expect for small $\delta\Omega$ that the total energy is of the form

$$E_T\approx E_T^0+\frac{F_1(n)}{2}\left[\frac{l}{a_\nu}\right]\left[\frac{\delta\Omega}{\Omega_\nu}\right]^2 -F_2(n)\left[\frac{\pi^2}{\alpha(\nu)\epsilon_{\rm VG}\nu}\right]\left[\frac{1}{n}\right]\left[\frac{\delta\Omega}{\Omega_\nu}\right]\ln(n) \ , \tag{4.14}$$

where E_T^0 is the energy of the undistorted lattice, F_1 and F_2 are constants of order 1 which depend on the lattice pattern, and the factor $\ln(n)$ is from the mean separation between positively charged sites. This energy is minimized by nonzero $\delta\Omega$. The magnitude of $\delta\Omega$ tends to be larger for larger n, where the Coulomb gas energy is larger, and for smaller ν, where the electrostatic energy is

relatively small. The dependence of the constants F_j on the crystal structure (n) is unimportant for large n.

However, for small n, which are the commensurabilities of interest, the vortex-gas ground states in general are not known, and in addition the ground-state configurations may not be compatible with the lattice distortions described above. For example, for $n=2$, we can find no pattern of lattice distortion which does not result in rather long-range electric fields For instance, one can form a striped phase, in which rows of plaquettes are alternately large and small. This pattern results in a permanent dipole moment in each unit cell, and hence is relatively less favorable energetically. Thus it appears that lattice distortion does not help stabilize the $n=2$ state very much. By contrast, for $n=3$ one can find a lattice pattern which is greatly stabilized by distortions. For example, by breaking the lattice up into hexagons which consist of six plaquettes, the energy can be reduced by contracting one third of the hexagons and expanding the other two thirds. However, it is not known whether this configuration actually corresponds to the vortex-gas ground state for $n=3$. Note also that by minimizing E_T in Eq. (4.14) with respect to $\delta\Omega$, we find a value of $\delta\Omega\sim\Omega_v$. From this we conclude (1) lattice distortion can be a very important source of stabilization of a phase, and (2) the small amplitude analysis of Eq. (4.14) is inadequate for treating the effect; energies must be computed for the distorted lattice itself. The details of this discussion are based on the notion of an underlying lattice. As is the case with our quasiparticles, we feel that the competition between local electrostatic and ring-exchange energies is a mechanism which is not sensitive to any underlying crystalline order.

Since the $\nu=\frac{1}{3}$ case is so much more stable (at least, in the absence of lattice distortions discussed above) than any other density, it is appealing to consider a hierarchy scheme analogous to that proposed by Haldane,[10] Halperin,[14] and Laughlin[20] in connection with Laughlin's ground states. In this scheme, the density is changed from $\nu=1/m$ by adding fractionally charged quasiparticles. When the density of quasiparticles is sufficient, one finds a new stable incompressible ground state in which the quasiparticles themselves have condensed into a Laughlin-type state. The generalization of this scheme to the cooperative ring-exchange formalism is straightforward. The density is changed from $\nu=1/m$ by adding quasiparticles and the contribution to the energy from cooperative ring exchanges of quasiparticles is calculated. The analysis proceeds as for the electrons, but with a renormalized tunneling coefficient α' and with fractional statistics,[13,14] appropriate for the fractionally charged quasiparticles. As in the usual hierarchy scheme, the quasiparticles are assumed to behave as particles with fractional charge, interacting via the Coulomb potential. In this case, α' is given by Eq. (2.32) but with $\nu\rightarrow\nu^*=m^2(\nu-1/m)$, where ν^* is the density of quasiparticles per "quasiflux quantum" $\phi_0^*=hc/Q^*=m\phi_0$.

As before, there are three contributions to the phase associated with a single cooperative ring exchange; these are the statistics phase, the Aharonov-Bohm phase, and the fluctuation determinant phase, which we will denote by θ_s, θ_A, and θ_D, respectively. The statistics phase is

$$\theta_s=\frac{1}{m}\sum_{\substack{i,j\\(i<j)}}\Delta\phi_{ij}$$
$$=\pm\frac{\pi}{m}(L-1)\pm\frac{2\pi}{m}N_{\rm qp}\ , \tag{4.15}$$

where $\Delta\phi_{ij}$ is the change of the azimuthal angle of particle i relative to particle j, L is the number of quasiparticles on the ring, $N_{\rm qp}$ is the number of quasiparticles enclosed by the ring and the $\pm$ refers to the direction of the exchange path. For the triangular lattice, this phase can be written as

$$\theta_s=\pm\frac{\pi}{m}N_A\pm\frac{\pi}{m}\ , \tag{4.16}$$

where N_A is the number of enclosed plaquettes. The Aharonov-Bohm phase is

$$\theta_A=\pm\frac{\pi N_A}{|\nu^*|}\ . \tag{4.17}$$

Therefore the contribution to the partition function from a single cooperative ring exchange involving L quasiparticles of charge $q^*=e/m$ is

$$\left[\frac{d\tau}{\tau_0'}\right]\exp\left[-\alpha'(\nu)L\pm i\pi N_A\left[\frac{1}{|\Delta\nu^*|}\pm\frac{1}{m}\right]\pm i\frac{\pi}{m}+i\theta_D\right]. \tag{4.18}$$

The requirement that rings of all sizes should add in phase produces an expression for the densities of possible incompressible states:

$$\frac{1}{|\nu_*|}\pm\frac{1}{m}=2n,\quad n=\pm1,\pm2,\ldots\ . \tag{4.19}$$

For example, from the $\nu=\frac{1}{3}$ state, one obtains the $\nu=\frac{2}{5},\frac{2}{7},\ldots$ states. There is, as before, a phase factor per ring of $\pm\pi/m+\theta_D$. In the case of fermions, we argued that $\theta_D=\pi$, and hence this factor is trivial. We do not have an analogous argument for particles with fractional statistics, although a statistics dependent phase θ_D is not ruled out. In fact, it has been suggested[47] that in the dense ring phase, a phase factor per loop simply renormalizes (increases) the effective α in the DG model.

We comment that it is possible that these two "hierarchy" schemes which we have discussed are equivalent. The distorted lattice in the first scheme looks like a lattice at some other density with quasiparticles on some fraction of the sites, which is precisely the second scheme. The difference between these two schemes though is that the first is an analysis done completely within the electron formalism and concentrates on static distortions of the lattice to relieve the frustration, while the second involves treating the quasiparticles as fundamental particles and looks at dynamic distortions (quasiparticle motions). Looking into the possible equivalence of these two

schemes could shed some light on why the usual hierarchy scheme appears to be valid even though one is pushing the quasiparticle concept well beyond its usual range of validity.

V. CONCLUSIONS

We have formulated a theory of ring-exchange condensation in an interacting two-dimensional electron gas at high magnetic field, which describes a transition (at zero temperature) from a low-density, sparse-ring phase to a higher-density ring condensate at a critical value of the Landau-level filling fraction, $\nu_c \approx \frac{1}{3}$. This phase transition is precipitated by a cooperative ring exchange (CRE) instability. A CRE event is one in which a set of electrons in the lattice, forming a ring, executes a cooperative motion, the result of which is a cyclic permutation of that set. Expressing the partition function as a sum over CRE events, we find that the individual terms will in general interfere randomly with one another unless the effective magnetic flux per plaquette, $f(\nu)=(\nu^{-1}-1)/2$, is a simple rational number. This effective flux accounts for both the Aharonov-Bohm phase incurred during a CRE motion *and* for the permutation signature that arises from Fermi statistics. The rings will contribute to the energy in a singular matter if the tunneling amplitude $e^{-\alpha(\nu)}$ is sufficiently large, and if the flux $f(\nu)$ is a simple rational value, which allows certain classes of rings to interfere constructively. We find that this exchange condensation, which produces an incompressible ground state and a cusp in the ground-state energy as a function of ν, is likely to occur in the vicinity of $\nu=\frac{1}{3}$, and possibly near other odd denominator rational filling fractions.

The CRE tunneling parameters are evaluated using a coherent-state path-integral formalism, which restricts the Hilbert space to the lowest Landau level. Unfortunately, there are several technical issues which cloud our theory at present. In particular, we do not yet properly understand the phase of the fluctuation prefactors emerging from the path integral. It is also unclear whether the spin models which we use for our analysis and which only approximately treat interactions between CRE events, retain enough validity in the dense-ring phase, where there is a substantial overlap of rings at any given time. These issues deserve more attention.

The CRE theory also implies the existence of fractionally charged quasiparticle excitations, with $e^*=\pm\nu_i e$ and where ν_i denotes one of the preferred rational filling fractions. The stability of these quasiparticles vanishes discontinuously as one proceeds into the sparse-ring phase. In addition, we have derived a Hamiltonian, $H_{\rm eff}$, which describes the coupling of ring-exchange processes and Wigner lattice magnetophonons. A naive expansion of $H_{\rm eff}$ to lowest order leads to a renormalized magnetophonon spectrum which obeys an acoustic dispersion $\omega_k \sim k$, at long wavelengths; the unrenormalized Wigner lattice magnetophonons satisfy $\omega_k \sim k^{3/2}$. There is good reason to question the validity of the naive expansion, and indeed previous theoretical[18] and numerical[15] results find a gap for the long-wavelength collective mode. We are currently attempting to treat collective excitations without linearizing the effective potential as in our present approach to these modes.

The cooperative ring-exchange approach emphasizes the importance of correlation between large numbers of electrons over large distances, as in critical phenomena. This view is in contrast with the numerical work based on Laughlin's wave function which emphasizes the importance of electron pair correlations at short distance. Nevertheless, the results of these apparently contradictory theories are quite similar. For example, both schemes lead to the incompressibility of the system at fractional densities $\nu_i=n/m$ with m and odd integer, fractionally charged quasiparticles, and a gap 2Δ in the quasiparticle spectrum. An important question is whether these theories describe the same underlying physics in different languages. While the Laughlin state

$$\psi_0=\prod_{\substack{i,j\\(i<j)}}(z_i-z_j)^m\exp\left[-\sum_k |z_k|^2/4\right] \tag{5.1}$$

features the pair correlation factor $(z_i-z_j)^m$, the product over i and j leads to correlations between chains or rings of particles; e.g., $(z_1-z_2)^m(z_2-z_3)^m(z_3-z_1)^m$ describes a three-particle ring correlation. Thus the peculiar properties of the 2D electron gas in a strong magnetic field may ultimately arise as described by the Laughlin state from the existence of such large rings which are implicitly contained in this function. The sharpness of the quantization of the magnetic densities $\nu_i=n/m$ suggests that large distance scales are involved, otherwise finite size fluctuation effects would appear to spoil this precise quantization. Unfortunately, we do not have a direct mathematical link between the Laughlin and CRE approaches, although we believe such a link may well exist. Recently Lee, Baskaran, and Kivelson[48] have demonstrated that the long-wavelength properties of Laughlin's ground state can be derived from a generalized CRE approach.

If in fact these two theories describe the same or closely related physics in two very different languages, does the CRE scheme give anything new beyond the Laughlin scheme? We believe the answer to this question is yes in that the CRE scheme is constructed to treat a continuous range of densities rather than only $\nu=n/m$ and its immediate vicinity. Thus, the CRE predicts the energy varies as $|\delta\nu|\ln|\delta\nu|$ for a spatially uniform deviation of ν from a magnetic value n/m. Since the chemical potential $\mu=\partial E/\partial\nu$ diverges for such uniform deviations, it follows that the extra charge can be accommodated at lower energy by clumping it up in quasiparticles of charge Q. The quantization of Q, for example $Q=\pm\nu_i e$ near density $\nu_i=1/m$, is a simple consequence of the condition that the energy of a quasiparticle be finite; other values of Q lead to divergent energies. The emphasis on long-range correlations also suggests that finite-size effects might be observed in the FQHE, as in critical phenomena. Whether periodic boundary conditions in model calculations eliminate such effects remains to be determined. In addition, certain calculations which emphasize long-range correlations may be easier to perform in the CRE language, as is the case using the renormalization-group techniques in critical-point problems. This raises the

question of whether there exists an effective-field theory which properly handles the CRE effects for long-wavelength properties. Indeed Girvin and MacDonald[49] have recently proposed a possible order parameter for the FQHE. Their work which is based on Laughlin's wave function, suggests a topological order parameter analogous to that of the two-dimensional XY model and, hence, further suggests a connection to the CRE theory.

While the above discussion of the CRE approach is developed in the context of an underlying Wigner lattice, fluctuation effects arising from CRE processes or other tunneling processes have a tendency to reduce the strength of crystalline order. It seems likely that for densities ν larger than the critical density ν_c for CRE to be effective, the lattice melts and forms a strongly correlated liquid. Whether or not this is the case, we believe that the CRE mechanism is operative and in no way depends on a charge-density wave ground state for its existence.

ACKNOWLEDGMENTS

We gratefully acknowledge useful conversations with G. Baskaran, A. J. Berlinsky, S. Chakravarty, F. D. M. Haldane, J. K. Jain, D. H. Lee, P. B. Littlewood, A. Luther, L. S. Schulman, D. Stroud, and D. J. Thouless. This work was supported in part by the National Science Foundation (NSF) through Grant Nos. DMR 82-16285 and DMR 83-18051. One of us (S.K.) acknowledges the hospitality of the Institute for Theoretical Physics, University of California, Santa Barbara (ITP-UCSB) where much of this work was carried out, and two of us (S.K. and J.R.S.) acknowledge the hospitality of Nordisk Institut for Teoretisk Atomfysik (NORDITA) where further work was completed. One of us (D.P.A.) acknowledges support by AT&T Bell Laboratories. Another of us (C.K.) was partly supported by the Canadian Natural Sciences and Engineering Research Council. One of us (S.K.) was partially supported by the Alfred P. Sloan Foundation.

APPENDIX A: THE PHASE OF THE PREFACTOR

In this appendix, we discuss the phase of the fluctuation determinant. It follows from the analysis of Sec. II C that in the dilute loop gas phase, ring exchanges lower the energy of the system at densities $\nu_m=(2m+1)^{-1}$ only if the fluctuation determinant for a single ring exchange is negative. If the determinant were positive, in the dilute regime, ring exchanges would increase the energy of the system at densities ν_m. In the dense-ring phase, it has been argued that independent of the sign of the fluctuation determinant, ring exchanges always lower the energy at such densities.[47] However, the critical value of α is smaller if the determinant is positive, and thus the very existence of a dense-ring phase is called into question. It is therefore necessary to determine the phase of the fluctuation determinant for a single ring exchange.

In the absence of a magnetic field the fermion ground state for a given real N-body Hamiltonian will lie at a higher energy than the corresponding unsymmetrized ground state. Furthermore, the sign of the contribution to the energy from a ring exchange involving L fermions can be shown to be positive for L even and negative for L odd.[50] This is a direct consequence of the well-known argument which shows that the (unrestricted) ground-state wave function has no nodes.[43] This argument, in turn, depends crucially on the kinetic piece of the Hamiltonian. In essence, any wave function which vanishes can lower its energy by reversing its sign in various regions (and rounding out the resulting cusp) so that it is always positive. By eliminating the nodes of the wave function, the kinetic energy is reduced. Although the potential energy is usually increased by this procedure (i.e., for repulsive interparticle interactions which fall off monotonically with distance, by eliminating modes at $r_i=r_j$, which are introduced through the antisymmetrization of the wave function, the potential energy is always increased), the change in the kinetic energy dominates.

In the presence of a magnetic field, the Hamiltonian is no longer real, and the usual analysis of the sign of exchange terms cannot be applied. A strong magnetic field has two effects on the sign: it introduces Aharonov-Bohm phases as the particles move around and it quantizes the kinetic energy, or, in the strong-field limit which we are considering, it quenches the kinetic energy. The first effect will obviously enter in the phase associated with a ring exchange. This phase is explicitly included in the action of the classical path and, at densities $\nu_m=(2m+1)^{-1}$, where there are an odd number of flux quanta per plaquette, it contributes a factor of $(-1)^L$ for a ring exchange involving L electrons. The form of the kinetic energy also has an important effect on the phase. The zero magnetic-field argument suggests that in a strong field the energy may be lowered by having as many nodes as possible along the lines where particles come together, $r_i=r_j$. Indeed, if the pair interaction is sufficiently short ranged, the Laughlin wave function, which has all nodes along such lines, is the exact, nondegenerate ground state of *arbitrary* permutation symmetry at density $\nu=1/m$.[52] If one assumes that it is energetically favorable for the many-particle wave function to vanish when two particles coincide, then one concludes that ring exchanges always lower the energy at densities $\nu_m=(2m+1)^{-1}$, in other words, that the fluctuation determinant must be negative for fermions.

If one calculates the contribution to the energy from pairwise ring exchange using the Maki-Zotos variational wave function, one finds that in the strong-field limit ring exchanges do always lower the energy at densities ν_m. Although one is not guaranteed of obtaining the correct sign for exchange contributions to the energy from calculating overlap integrals using a variational wave function, since the Maki-Zotos wave function is the starting point for our analysis, it is consistent to use the sign obtained from it.

The fluctuation prefactor has been further investigated by Jain and Kivelson,[28] who considered a single-particle model in a strong magnetic field, in which the particle hops between sites equally spaced along a ring of radius r_0. By choosing a sufficiently simple model potential, the classical action may be evaluated analytically and the fluctuation prefactor then extracted by comparing the separation of low-lying energy levels (obtained by numerical

solution of the projected Schrödinger equation) to e^{-S_c}. Jain and Kivelson postulated that, in the large r_0 limit, the phase of the prefactor tends to the value $e^{i\pi/n}$, where n is the number of tunneling centers along the ring. Numerical results have thus far confirmed this speculation, although only the cases $n=2$ and $n=4$ have been studied. As applied to our ring exchange theory, this result seems to imply that a factor of -1 *per ring* arises from the fluctuation prefactor.

APPENDIX B: SINGLE-PARTICLE BASIS

In this appendix, we discuss a continuous representation for the single-particle basis spanning a given Landau level. The bulk of the discussion relies on many well-known results, which we now summarize.

1. Cyclotron and guiding center variables

The dynamics of a two-dimensional system in the presence of a uniform magnetic field $B=-B_0\hat{\mathbf{z}}$ may be separated into two distinct motions, cyclotron and guiding center motion. Working in the symmetric gauge, where the vector potential is $A_i=\frac{1}{2}B_0\epsilon_{ij}r_j$, the cyclotron position and momentum are given by

$$\xi_i=\tfrac{1}{2}r_i-\frac{l^2}{\hbar}\epsilon_{ij}p_j \ , \tag{B1a}$$

$$\pi_i=p_i+\frac{\hbar}{2l^2}\epsilon_{ij}r_j$$

$$=\frac{\hbar}{l^2}\epsilon_i\xi_j \ , \tag{B1b}$$

while the corresponding guiding center variables are

$$\wp_i=\tfrac{1}{2}r_i+\frac{l^2}{\hbar}\epsilon_{ij}p_j \ , \tag{B2a}$$

$$\kappa_i=p_i-\frac{\hbar}{2l^2}\epsilon_{ij}r_j$$

$$=-\frac{\hbar}{l^2}\epsilon_{ij}\wp_j \ . \tag{B2b}$$

These (independent) pairs satisfy the canonical commutation relations $[\pi_i,\xi_j]=[\kappa_i,\wp_j]=-i\hbar\delta_{ij}$, with no other nonzero commutators. The free-particle Hamiltonian is

$$H_0=\frac{1}{2m}\pi_i\pi_i \ . \tag{B3}$$

(Throughout the discussion, two-dimensional vectors will be indexed by Roman labels, and ϵ_{ij} will denote the antisymmetric tensor of rank two, with $\epsilon_{12}=+1$.) The magnetic length is $l=\sqrt{\hbar c/eB}$.

One may now define the independent oscillator ladder operators in terms of the complex coordinates $z=x+iy$ and $\bar{z}=x-iy$:

$$a=(\xi_x+i\xi_y)/\sqrt{2}l$$

$$=\sqrt{2}l\left[\bar{\partial}+\frac{1}{4l^2}z\right] \ , \tag{B4a}$$

$$b=(\wp_x-i\wp_y)/\sqrt{2}l$$

$$=\sqrt{2}l\left[\partial+\frac{1}{4l^2}\bar{z}\right] \ , \tag{B4b}$$

which obey $[a,a^\dagger]=[b,b^\dagger]=1$. The Hamiltonian H_0 becomes

$$H_0=\hbar\omega_c(a^\dagger a+\tfrac{1}{2}) \ , \tag{B5}$$

with $\omega_c=eB/mc$, the cyclotron frequency. The $(a,a^\dagger)$ pair are *inter*-Landau-level operators which connect states of different energy (odd multiples of $\frac{1}{2}\hbar\omega_c$) Since H_0 is cyclic in the *intra*-Landau-level operators $(b,b^\dagger)$, there is no natural frequency associated with them, and their application connects different elements of a degenerate set of states. This Landau-level degeneracy is extensive, with the total number of such states per unit area given by $N_L/\Omega=B/\phi_0=1/2\pi l^2$.

2. Basis states

The normalized fiducial state, $|0,0\rangle$, defined by $a\,|0,0\rangle=b\,|0,0\rangle=0$, possesses the real space representation

$$\psi_{00}(\bar{z},z)=\langle\mathbf{r}\,|\,0,0\rangle=\frac{1}{(2\pi l^2)^{1/2}}e^{-z\bar{z}/4l^2} \ . \tag{B6}$$

Construction of the usual Fock space of state vectors proceeds by application of the raising operators $a^\dagger$ and $b^\dagger$:

$$|\,m,n\,\rangle=\frac{(a^\dagger)^n}{\sqrt{n!}}\frac{(b^\dagger)^m}{\sqrt{m!}}\,|\,0,0\rangle \ , \tag{B7a}$$

$$\langle\,m',n'\,|\,m,n\,\rangle=\delta_{mm'}\delta_{nn'} \ , \tag{B7b}$$

$$\psi_{mn}(\bar{z},z)=(-1)^n\left[\frac{n!}{2\pi l^2 m!}\right]^{1/2}\left[\frac{z}{\sqrt{2}l}\right]^{m-n}$$

$$\times L_n^{m-n}(\bar{z}z/2l^2)e^{-\bar{z}z/4l^2} \ , \tag{B7c}$$

where $L_j^k(x)$ is a Laguerre polynomial. This is the often-used "angular momentum basis," so named because the elements $|\,m,n\,\rangle$ are eigenstates of the angular momentum operator,

$$L_z=\epsilon_{ij}r_ip_j$$

$$=\hbar(b^\dagger b-a^\dagger a) \ . \tag{B8}$$

Next, we introduce the normalized coherent state,

$$|\,\mathbf{R},n\,\rangle=\frac{(a^\dagger)^n}{\sqrt{n!}}e^{(\bar{R}b^\dagger-Rb)/\sqrt{2}l}\,|\,0,0\rangle \ , \tag{B9a}$$

which is radially localized about the guiding center $\mathbf{R}$:

$$\phi_{\mathbf{R},n}=\frac{1}{(2\pi l^2 n!)^{1/2}}\left[\frac{\bar{z}-\bar{R}}{\sqrt{2}l}\right]^n e^{(z\bar{R}-\bar{z}R)/4l^2}e^{-|z-R|^2/4l^2} \ , \tag{B9b}$$

with $R=R_x+iR_y$, etc. The coherent-state overlap is given by

$$\langle\,\mathbf{R}',n'\,|\,\mathbf{R},n\,\rangle=\delta_{nn'}e^{(R'\bar{R}-R\bar{R}')/4l^2}e^{-|R-R'|^2/4l^2} \ . \tag{B10}$$

We stress that we are dealing with a continuous representation here; the coherent states are eigenstates of the non-Hermitian operator b, with $b\,|\,\mathbf{R},n\rangle=(\bar{R}/\sqrt{2}l)\,|\,\mathbf{R},n\rangle$, and thus they are *not* orthogonal. Nevertheless, the projector P_n onto a given Landau level takes a simple form:

$$P_n=\sum_{m=-\infty}^{\infty}|\,m,n\rangle\langle m,n\,| =\int\frac{d^2R}{2\pi l^2}\,|\,\mathbf{R},n\rangle\langle\mathbf{R},n\,|\ . \tag{B11}$$

In the lowest Landau level ($n=0$), the above formulas can be summarized (dropping the $n=0$ index):

$$\phi_{\mathbf{R}}(\mathbf{r})=\frac{1}{(2\pi l^2)^{1/2}}e^{-i\mathbf{r}\times\mathbf{R}\cdot\hat{\mathbf{z}}/2l^2}e^{-(\mathbf{r}-\mathbf{R})^2/4l^2}\ , \tag{B12a}$$

$$\langle\mathbf{R}'\,|\,\mathbf{R}\rangle=e^{-i\mathbf{R}'\times\mathbf{R}\cdot\hat{\mathbf{z}}/2l^2}e^{-(\mathbf{R}-\mathbf{R}')^2/4l^2}\ , \tag{B12b}$$

$$P_n=\int\frac{d^2R}{2\pi l^2}\,|\,\mathbf{R}\rangle\langle\mathbf{R}\,|\ . \tag{B12c}$$

APPENDIX C: COHERENT-STATE PATH INTEGRATION

The usual procedure by which the imaginary time propagator $\langle x'\,|\,e^{-\beta H}\,|\,x''\rangle$ is transcribed over to a path integral entails dividing the inverse temperature β into a large number of equal intervals of size ε, and subsequently inserting a resolution of unity, $\mathbb{1}=\int dx\,|\,x\rangle\langle x\,|$, at each step. In any physical context, the expression $\mathbb{1}$ always represents a projector onto a relevant subspace, the states $|\,x\rangle$ likewise so restricted. Using the coherent-state basis and projector discussed in Appendix B, a coherent-state path integral can be derived for the propagator. In this appendix, we shall discuss the essential features of this formalism, including the method of steepest descents approximation (SDA). The treatment follows that of Schulman[26] and Girvin and Jach.[51]

1. Single-body path integral

The matrix element $\langle\mathbf{R}_f\,|\,e^{-\beta V}\,|\,\mathbf{R}_i\rangle$ is written

$$\begin{aligned}\langle\mathbf{R}_f\,|\,e^{-\beta V}\,|\,\mathbf{R}_i\rangle&=\int\frac{d^2R_1}{2\pi l^2}\cdots\int\frac{d^2R_M}{2\pi l^2}\langle\mathbf{R}_f\,|\,e^{-\beta V}\,|\,\mathbf{R}_M\rangle\cdots\langle\mathbf{R}_1\,|\,e^{-\beta V}\,|\,\mathbf{R}_i\rangle\\&=\int\prod_{k=1}^{M}\frac{d^2R_k}{2\pi l^2}e^{-S_M[\mathbf{R}]}+O(\varepsilon^2)\ ,\end{aligned} \tag{C1}$$

$$S_M[\mathbf{R}]=\frac{1}{4l^2}\sum_{j=0}^{M}[R_{j+1}(\bar{R}_{j+1}-\bar{R}_j)-\bar{R}_j(R_{j+1}-R_j)]+\varepsilon\sum_{j=0}^{M}\tilde{V}(\mathbf{R}_{j+1}\,|\,\mathbf{R}_j)\ ,$$

with

$$\begin{aligned}\tilde{V}(\mathbf{R}'\,|\,\mathbf{R})&=\langle\mathbf{R}'\,|\,V\,|\,\mathbf{R}\rangle/\langle\mathbf{R}'\,|\,\mathbf{R}\rangle\\&=\tilde{V}(R'\,|\,\bar{R})\ .\end{aligned} \tag{C2}$$

As mentioned in the text, the continuum limit of this path integral is not well defined. The origin of the difficulty is the nonorthogonality of the basis states $|\,\mathbf{R}\rangle$. Whereas the usual quantum mechanical propagator approaches a δ function in the zero time limit, e.g.,

$$\lim_{t\to 0}\langle x'\,|\,e^{-iHt/\hbar}\,|\,x\rangle=\delta(x-x')\ ,$$

the coherent-state propagator tends to the overlap

$$\langle\mathbf{R}'\,|\,\mathbf{R}\rangle=e^{-i\mathbf{R}'\times\mathbf{R}\cdot\hat{\mathbf{z}}/2l^2}e^{-(\mathbf{R}-\mathbf{R}')^2/4l^2}\ ,$$

and there is thus a nonzero probability for the particle to undergo an instantaneous hop over an arbitrary distance. This is reflected in the fact that the continuous time limit ($\varepsilon\to 0$) of the coherent-state action functional,

$$\begin{aligned}S[\mathbf{R}(\tau)]=&\frac{1}{4l^2}[\bar{R}_i(R_i-R(0))+R_f(\bar{R}_f-\bar{R}(\beta))]\\&+\int_0^\beta d\tau\left[\frac{1}{4l^2}(R\dot{\bar{R}}-\bar{R}\dot{R})+\tilde{V}(R\,|\,\bar{R})\right]\end{aligned} \tag{C3}$$

is *linear* in time derivatives, and thus discontinuous paths have finite action. This, in turn, implies that the $\varepsilon\to 0$ limit of the coherent-state path integral,

$$\langle\mathbf{R}_f\,|\,e^{-\beta V}\,|\,\mathbf{R}_i\rangle=\int_{\substack{\bar{R}(0)=\bar{R}_i\\R(\beta)=R_f}}\mathcal{D}[\mathbf{R}(\tau)]e^{-S[\mathbf{R}(\tau)]} \tag{C4}$$

is dominated by discontinuous paths, and indeed the limit is ill defined. In general, one must either work with the discrete-time path integral, or use some other procedure to make (C4) well defined (see below). Fortunately, we are only interested in the semiclassical limit when $\tilde{V}(\bar{R})$ is a slowly varying function of its argument over the length scale l, and we can employ the SDA to evaluate the path integral. The path which extremizes the discrete time action satisfies the discrete-time classical equations of motion

$$\begin{aligned}\bar{R}_j-\bar{R}_{j-1}&=-2l^2\varepsilon\frac{\partial}{\partial R_j}\tilde{V}(R_j\,|\,\bar{R}_{j-1})\ ,\\R_{j+1}-R_j&=+2l^2\varepsilon\frac{\partial}{\partial\bar{R}_j}\tilde{V}(R_{j+1}\,|\,\bar{R}_j)\ ,\end{aligned} \tag{C5}$$

with $j=1,\ldots,M$. From these equations, one sees that the $\{\bar{R}_j\}$ are evolved *forward* from initial data $\bar{R}_0=\bar{R}_i$, while the $\{R_j\}$ are evolved *backward* from final data $R_{M+1}=R_f$; the differences $R_0^{\mathrm{SDA}}-R_i$ and $\bar{R}_{M+1}^{\mathrm{SDA}}-\bar{R}_f$ are *not*, in general, infinitesimals. It is therefore convenient to write

$$S_M[\mathbf{R}]=\frac{1}{4l^2}[\bar{R}_0(R_0-R_1)+R_{M+1}(\bar{R}_{M+1}-\bar{R}_M)]+\frac{1}{4l^2}\sum_{j=1}^{M}[R_j(\bar{R}_j-\bar{R}_{j-1})-\bar{R}_j(R_{j+1}-R_j)]+\varepsilon\sum_{j=0}^{M}\tilde{V}(R_{j+1}\mid\bar{R}_j)\ . \tag{C6}$$

For sufficiently small ε, and whenever the classical path is discontinuous, the discrete-time classical equations of motion can be replaced by their continuous time limit:

$$\dot{\bar{R}}=-2l^2\frac{\partial}{\partial R}\tilde{V}(R\mid\bar{R})\ ,\qquad \dot{R}=+2l^2\frac{\partial}{\partial\bar{R}}\tilde{V}(R\mid\bar{R})\ , \tag{C7}$$

supplemented by the boundary conditions $R(\beta)=R_f$, $\bar{R}(0)=\bar{R}_i$. The classical paths may be well defined in the small ε limit.

Caution must be exercised in extending the above formalism toward evaluating the single-body partition function,

$$Z_1=\int\frac{d^2R}{2\pi l^2}\langle\mathbf{R}\mid e^{-\beta V}\mid\mathbf{R}\rangle\ , \tag{C8}$$

for the SDA equations may have no continuous solutions. The trouble arises from the boundary conditions that must be employed when integrating over the endpoints in Eq. (C8). In this case, the periodic boundary conditions $\bar{R}(\beta)=\bar{R}(0)$ and $R(\beta)=R(0)$ must be applied to the *first*-order equations of motion in Eqs. (C7a) and (C7b). Such a system need not possess a solution, and the best that one can do is to satisfy the Euler-Lagrange equations *locally,* while admitting discontinuities at certain points along the path. (As discussed in the body of the paper, these problems do not arise for our ring-exchange paths.) We shall return to the issue of path discontinuities at the end of this appendix.

2. Many-body path integral

The derivation of the many-body path integral directly parallels that for the single-body problem. In what follows, we shall denote by $\mathbf{R}_i^a$ the guiding center of particle i ($1\le i\le N$) at (imaginary) time $\tau=a\varepsilon$, and by $\mathcal{R}$ the collection of coordinates $(\mathbf{R}_1,\ldots,\mathbf{R}_N)$.

The imaginary time propagator is given by

$$\langle\mathcal{R}''\mid e^{-\beta\mathcal{V}}\mid\mathcal{R}'\rangle=\int\prod_{i=1}^{n}\prod_{a=1}^{M}\frac{d^2R_i^a}{2\pi l^2}e^{-S_M[\mathcal{R}]}+O(\varepsilon^2)\ , \tag{C9}$$

where the discretized action is

$$S_M[\mathcal{R}]=\sum_{a=0}^{M}\left[\sum_{i=1}^{N}\frac{1}{4l^2}[R_i^{a+1}(\bar{R}_i^{a+1}-\bar{R}_i^a)-\bar{R}_i^a(R_i^{a+1}-R_i^a)]+\tfrac{1}{2}\varepsilon\sum_{\substack{i,j\\(i\neq j)}}^{N}\tilde{V}_2(R_i^{a+1},R_j^{a+1}\mid\bar{R}_j^a,\bar{R}_i^a)\right]\ . \tag{C10}$$

The potential is written as a sum of two-body terms:

$$\mathcal{V}(\mathbf{r}_1,\ldots,\mathbf{r}_N)=\tfrac{1}{2}\sum_{\substack{i,j\\(i\neq j)}}^{N}V_2(\mathbf{r}_i-\mathbf{r}_j)\ ,$$
$$\tilde{V}_2(R',Q'\mid\bar{Q},\bar{R})=\langle\mathbf{R}',\mathbf{Q}'\mid V_2\mid\mathbf{R},\mathbf{Q}\rangle/\langle\mathbf{R}'\mid\mathbf{R}\rangle\langle\mathbf{Q}'\mid\mathbf{Q}\rangle\ . \tag{C11}$$

The SDA equations of motion are

$$\bar{R}_i^a-\bar{R}_i^{a-1}=-2l^2\varepsilon\frac{\partial}{\partial R_i^a}\sum_{j=1}^{N}\tilde{V}_2(R_i^a,R_j^a\mid\bar{R}_j^{a-1},\bar{R}_i^{a-1})\ ,$$
$$R_i^{a+1}-\bar{R}_i^a=+2l^2\varepsilon\frac{\partial}{\partial\bar{R}_i^a}\sum_{j=1}^{N}\tilde{V}_2(R_i^{a+1},R_j^{a+1}\mid\bar{R}_j^a,\bar{R}_i^a)\ , \tag{C12}$$

with $a=1,\ldots,M$, and subject to the boundary conditions $\bar{R}_i^0=\bar{R}_i'$ and $R_i^{M+1}=R_i''$.

In the continuous time limit, the many-body path integral reduces to

$$\langle\mathcal{R}''\mid e^{-\beta\mathcal{V}}\mid\mathcal{R}'\rangle=\int_{\substack{\bar{R}_i(0)=\bar{R}_i'\\R_i(\beta)=R_i''}}\mathcal{D}[\mathcal{R}(\tau)]e^{-S[\mathcal{R}(\tau)]}\ , \tag{C13}$$

where the continuous-time action is

$$S[\mathcal{R}(\tau)]=\sum_{i=1}^{N}\frac{1}{4l^2}\{\bar{R}_i'[R_i'-R_i(0)]+R_i''[\bar{R}_i''-\bar{R}_i(\beta)]\}+\int_0^\beta d\tau\left[\sum_{i=1}^{N}\frac{1}{4l^2}(R_i\dot{\bar{R}}_i-\bar{R}_i\dot{R}_i)+\tfrac{1}{2}\sum_{\substack{i,j\\(i\neq j)}}^{N}\tilde{V}_2(R_i,R_j\mid\bar{R}_j,\bar{R}_i)\right]\ . \tag{C14}$$

The SDA equations of motion are then

$$\dot{\bar{R}}_i=-2l^2\frac{\partial}{\partial R_i}\tilde{\mathcal{V}}[\mathcal{R}]\ ,\qquad \dot{R}_i=+2l^2\frac{\partial}{\partial\bar{R}_i}\tilde{\mathcal{V}}[\mathcal{R}]\ . \tag{C15}$$

The N-fermion partition function, Z_N, may now be cast into the form

$$Z_N=\frac{1}{N!}\sum_{\sigma\in S_N}\mathrm{sgn}(\sigma)\int\prod_{i=1}^{N}\frac{d^2R_i}{2\pi l^2}\langle\mathbf{R}_{\sigma(1)},\ldots,\mathbf{R}_{\sigma(N)}\,|\,e^{-\beta\mathcal{V}}\,|\,\mathbf{R}_1,\ldots,\mathbf{R}_N\rangle$$
$$=\frac{1}{N!}\sum_{\sigma\in S_N}\mathrm{sgn}(\sigma)\int_{\mathrm{traj}(\sigma)}\mathcal{D}[\mathcal{R}(\tau)]\exp\left[-\int_0^\beta d\tau\left[\sum_{i=1}^{N}\frac{1}{4l^2}(R_i\dot{\bar{R}}_i-\bar{R}_i\dot{R}_i)+\tfrac{1}{2}\sum_{\substack{i,j\\(i\neq j)}}\tilde{V}_2(R_i,R_j\,|\,\bar{R}_j,\bar{R}_i)\right]\right],\quad\text{(C16)}$$

where the boundary conditions require that $\bar{R}_{\sigma(i)}(\beta)=\bar{R}_i(0)$ and $R_{\sigma(i)}(\beta)=R_i(0)$. Again, the first-order equations of Eq. (C15) will in general be incompatible with the imposition of this periodicity constraint. For reference, the diagonal coherent-state matrix elements of the Coulomb potential $V_2(\mathbf{r})=e^2/\epsilon\mathbf{r}$ are

$$\tilde{V}_2(R,Q\,|\,\bar{Q},\bar{R})=\frac{\sqrt{\pi}e^2}{2\epsilon l}e^{-|R-Q|^2/8l^2}I_0(|R-Q|^2/8l^2)\,,\quad\text{(C17)}$$

where $I_0(x)$ is the modified Bessel function of the first kind.

3. Discontinuous paths

The presence of discontinuous paths implies that the naive continuous time limit of the discrete-time coherent-state path integral is not well defined. The discontinuous paths still show up in the continuous-time path integral since the action has only a term *linear* in the time derivative; there is no kinetic energy term quadratic in the time derivative to force continuity of the paths. However, the weight of discontinuous paths is not necessarily the same in the discrete-time and continuous-time formulations of the problem.

This problem is not of central importance to us here since, as discussed previously, in the $\epsilon\to 0$ limit, the classical paths tend to a smooth path, with possible discontinuities arising at the endpoints. Thus, the continuous-time formulation can be used to calculate the properties of the classical paths, but the prefactor, which we do not compute explicitly (except in the case of a displaced line), must be computed using the discrete-time formalism. Alternatively, Klauder[27] has shown that the coherent-state path integral can be defined by introducing an artificial kinetic energy term in the action, and then taking the limit as $m^*\to 0$ at the end of the calculation. Again, this procedure is only necessary when computing the prefactor.

Even with one of these prescriptions for computing the prefactor, there remains an ambiguity. The potential term in the continuous-time action is not uniquely specified since $\tilde{V}(\bar{z}_{j+1}\,|\,z_j)$ does not approach any function of z_j and $\bar{z}_j$ alone as $\epsilon\to 0$. In Eq. (C7) we made the replacement $V(\bar{z}_{j+1}\,|\,z_j)\to V(\bar{z}_j\,|\,z_j)$. Since $\bar{z}_{j+1}-\bar{z}_j$ is typically of order l, we could equally well have used any function of the form $V(\bar{z}\,|\,z)[1+O(l^2/R^2)]$, where R is the characteristic distance over which V varies. (By definition, $l/R\ll 1$ where the semiclassical approximation is valid.) Schulman has suggested that this ambiquity is related to operator order ambiquities in the original formulation. However, Klauder has shown (for polynomial potentials) that if one uses the prescription of taking the $m^*\to 0$ limit, the same propagator is obtained whether one chooses the potential term to be $V(\mathbf{R})$ directly, or, as we have done, its matrix elements $\tilde{V}(\mathbf{R})=\langle\mathbf{R}\,|\,V\,|\,\mathbf{R}\rangle$.

APPENDIX D: ACTION FOR A DISPLACED LINE

Imagine the simplest possible exchange path, namely that of a uniformly shifting line of charges within the Wigner crystal. When the line $\mathcal{L}$ is displaced, we have $\mathbf{R}_i=\mathbf{T}_i+\mathbf{a}\delta_{i\in\mathcal{L}}$, with $\delta_{i\in\mathcal{L}}$ unity if and only if lattice site i lies on the line in question. The matrix element of the Coulomb potential between coherent states was given in Appendix C:

$$V(\mathbf{R})=\frac{\sqrt{\pi}e^2}{2\epsilon l}e^{-R^2/8l^2}I_0(R^2/8l^2)\,.\quad\text{(D1)}$$

Accordingly, the energy of the displaced line configuration relative to that of the perfect Wigner crystal is

$$\Delta E=\sum_{(i,j)}[V(\mathbf{R}_i-\mathbf{R}_j)-V(\mathbf{T}_i-\mathbf{T}_j)]\,.\quad\text{(D2)}$$

The sum is broken up into three terms. The first term includes all pairs (i,j) in which both sites i and j lie off the line. This contribution to ΔE is obviously zero. The second term involves all pairs (i,j) where one of the sites, say i, is on the line and the other, j, is off:

$$\Delta E_2=\sum_{\substack{i\in\mathcal{L}\\ j\notin\mathcal{L}}}[V(\mathbf{T}_i+\mathbf{a}-\mathbf{T}_j)-V(\mathbf{T}_i-\mathbf{T}_j)]\,.\quad\text{(D3)}$$

Clearly the line energy is extensive, hence the energy per tunneling electron can be written

$$U(\mathbf{a})\equiv\Delta E_2/N_{\mathrm{line}}=\sum_{j\notin\mathcal{L}}[V(\mathbf{T}_j-\mathbf{a})-V(\mathbf{T}_j)]\,,\quad\text{(D4)}$$

where we have chosen the origin to lie on the line. The sum over j can in turn be written conveniently as a sum over *all* lattice sites minus a piece with $j\in\mathcal{L}$. The third and final term is, of course, that arising from both i and j on the line. *Since the tunneling is cooperative, this contribution to the classical action vanishes.*

We therefore find $U(\mathbf{a})=\delta\varepsilon_{\mathrm{all}}-\delta\varepsilon_{\mathrm{on}}$. The slowly convergent sum for $\delta\varepsilon_{\mathrm{all}}$ can be converted into a rapidly convergent sum by means of the Poisson summation formula,

$$\sum_T\delta(\mathbf{r}-\mathbf{T})=\frac{1}{\Omega_v}\sum_{\mathbf{G}}e^{i\mathbf{G}\cdot\mathbf{r}}\,,\quad\text{(D5)}$$

and the result is

$$\delta\varepsilon_{\rm all}=\frac{\nu e^2}{\epsilon l}\sum_{\substack{\mathbf{G}\\ \mathbf{G}\neq 0}}\frac{1}{|\mathbf{G}l|}e^{-\mathbf{G}^2l^2}(e^{-i\mathbf{G}\cdot\mathbf{a}}-1)\ . \tag{D6}$$

In the above formulas, $\mathbf{T}$ and $\mathbf{G}$ denote vectors in the direct and reciprocal lattices, respectively; $\Omega_\nu=2\pi l^2/\nu$ is the Wigner-Seitz cell area.

The identical technique may be applied to the "on" sum: Simply sum over all direct lattice vectors, but include, in an integral representation, a Kronecker δ function which enforces the online restriction. One finds

$$\delta\varepsilon_{\rm on}=\frac{\nu e^2}{\epsilon l}\sum_{\substack{\mathbf{G}\\ \mathbf{G}\neq 0}}\int_{-\pi}^{\pi}\frac{dc}{2\pi}\frac{1}{|\mathbf{G}l+c\mathbf{g}l|}\times e^{-(\mathbf{G}+c\mathbf{g})^2l^2}(e^{-i(\mathbf{G}+c\mathbf{g})\cdot\mathbf{a}}-1)\ , \tag{D7}$$

with $\mathbf{g}=2\hat{\mathbf{y}}/\sqrt{3}a_\nu$. While the virtue of Eq. (D7) is its rapid convergence, the integration complicates the numerical evaluation, and in practice it is more convenient to calculate the slowly converging expression

$$\delta\varepsilon_{\rm on}=\frac{\sqrt{\pi}e^2}{2\epsilon l}\sum_{\mathbf{T}\in\mathcal{L}}\{e^{-(\mathbf{T}-\mathbf{a})^2/8l^2}I_0[(\mathbf{T}-\mathbf{a})^2/8l^2]-e^{-T^2/8l^2}I_0(T^2/8l^2)\}\ . \tag{D8}$$

APPENDIX E: EQUIVALENT MODELS

In this appendix, we review the equivalences between the discrete Gaussian model, the XY model and the spin-wave–vortex-gas system. The frustrated XY model is described by the Hamiltonian

$$H=K\sum_{\langle \mathbf{r},\mathbf{r}'\rangle}[1-\cos(\theta_r-\theta_r'-A_{rr'})]\ , \tag{E1}$$

where the dynamical variables are the angles $\{\theta_r\}$ and the sum is over all nearest-neighbor pairs $\langle \mathbf{r},\mathbf{r}'\rangle$ on some lattice $\mathcal{L}$. This model has been used to describe Josephson-junction arrays in a transverse magnetic field,[38] where superconducting islands interact via a proximity coupling. The vector potential $A_{rr'}$ lives on the links of $\mathcal{L}$ and is constrained by the requirement that the integral $\oint\mathbf{A}\cdot d\boldsymbol{l}$ around a plaquette yield the total magnetic flux through that plaquette, which is written as $2\pi f$ in units of the superconducting flux quantum: $\sum_{\rm plaquette}A_{rr'}=2\pi f$, with $A_{rr'}\equiv(e^*/\hbar c)\int_r^{r'}\mathbf{A}\cdot d\boldsymbol{l}$, and $e^*=2e$ (the charge of the Cooper pair). Following José *et al.*,[44] consider a general Hamiltonian of the form

$$H[\{\theta_r\}]=-\sum_{\langle \mathbf{r},\mathbf{r}'\rangle}V(\theta_r-\theta_r'-A_{rr'})\ . \tag{E2}$$

The function $V(\theta)$ is assumed to be periodic, and may be expressed as a Fourier sum,

$$e^{V(\theta)}=\sum_{S=-\infty}^{\infty}e^{is\theta}e^{\tilde{V}(s)}\ . \tag{E3}$$

The partition function may then be written as

$$Z=\int\prod_{\mathbf{r}''}d\theta_{\mathbf{r}''}\prod_{\langle \mathbf{r},\mathbf{r}'\rangle}\sum_{S_{rr'}=-\infty}^{\infty}\exp[\tilde{V}(S_{rr'})+iS_{rr'}(\theta_r-\theta_{r'}-A_{rr'})]\ . \tag{E4}$$

To each distinct nearest neighbor pair $\langle \mathbf{r},\mathbf{r}'\rangle$ on $\mathcal{L}$ one associates a directed line from $\mathbf{r}$ to $\mathbf{r}'$. The bond spin $S_{rr'}$ is then written as the difference of nearest-neighbor-site spins $\mathbf{R}$ and $\mathbf{R}'$ on the dual lattice $\mathcal{L}^D$, where the segment from $\mathbf{R}$ to $\mathbf{R}'$ intersects that from $\mathbf{r}$ to $\mathbf{r}'$ such that $(\mathbf{r}'-\mathbf{r})\times(\mathbf{R}'-\mathbf{R})\cdot\hat{\mathbf{z}}>0$. This assignment satisfies the "zero divergence" constraint that arises from the $\{\theta_r\}$ integrations. Lastly, the vector potential term on $\mathcal{L}$ gives rise to a uniform imaginary field on $\mathcal{L}^D$, and the duality transformed partition function takes the form

$$Z=\mathrm{Tr}\,e^{-H[\{S_R\}]}\ ,\qquad H[\{S_{\mathbf{R}}\}]=-\sum_{\langle \mathbf{R},\mathbf{R}'\rangle}\tilde{V}(S_{\mathbf{R}}-S_{\mathbf{R}'})+2\pi if\sum_{\mathbf{R}}S_{\mathbf{R}}\ , \tag{E5}$$

which is a generalization of the DG model. To recover the DG Hamiltonian, we make use of the following approximation, valid for large K:

$$e^{K(\cos\theta-1)}\simeq\mathcal{N}\sum_{m=-\infty}^{\infty}e^{-(1/2)K_V(\theta-2\pi m)^2}\ . \tag{E6}$$

The value of the normalization constant $\mathcal{N}$ as well as the functional form of the Villain coupling $K_V(K)$ are determined by matching the values of the left- and right-hand sides of the above equation, as well as their second derivatives, at $\theta=0$. One finds that for $K>(2\pi)^{-1}$, $K_V\simeq K$ is a good approximation. The function $\tilde{V}(S)$ then becomes $\tilde{V}_V(S)=-S^2/2K_V$, which completes the mapping to the DG model. If $\mathcal{L}$ is a triangular lattice, then $\mathcal{L}^D$ is a honeycomb lattice.

The transformation to the spin-wave–vortex-gas system is even simpler, and follows directly from application of the Poisson summation formula

$$\sum_{n=-\infty}^{\infty}\delta(S-n)=\sum_{m=-\infty}^{\infty}e^{2\pi imS}\ . \tag{E7}$$

Inserting such a term for each dual lattice spin S_i, the trace over all integer S_i can be replaced by a product of integrals:

$$
\begin{aligned}
Z_{\mathrm{DG}} &= \sum_{\{S_i\}} \exp\left[-\alpha \sum_{\langle i,j\rangle} (S_i - S_j)^2 - 2\pi i \sum_k f_k S_k\right] \\
&= \int_{-\infty}^{\infty} \prod_i dS_i \prod_j \sum_{n_j=-\infty}^{\infty} \delta(S_j - n_j) \exp\left[-\alpha \sum_{\langle i,j\rangle} (S_i - S_j)^2 - 2\pi i \sum_k f_k S_k\right] \\
&= \sum_{\{m_i\}} \int_{-\infty}^{\infty} \prod_i dS_i \exp\left[-\alpha \sum_{i,j} S_i \mathcal{G}_{ij}^{-1} S_j + 2\pi i \sum_k S_k (m_k - f_k)\right] \\
&= Z_{\mathrm{SW}} Z_{\mathrm{VG}} \ . \qquad \text{(E8)}
\end{aligned}
$$

We have implicitly defined the lattice Green's function $\mathcal{G}_{ij}$, which is discussed in more detail in Appendix F. Our coupling α is related to the Villain constant by $\alpha = 1/2K_V$. The spin-wave partition function is trivial and results from an unconstrained trace over the Gaussian Hamiltonian H_{SW}:

$$
\begin{aligned}
H_{\mathrm{SW}} &= \alpha \sum_{\langle i,j\rangle} (\phi_i - \phi_j)^2 \ , \\
Z_{\mathrm{SW}} &= \int_{-\infty}^{\infty} \prod_i d\phi_k e^{-H[\{\phi_i\}]} \\
&= \exp\left[\tfrac{1}{2} N \Omega \int \frac{d^2k}{(2\pi)^2} \ln\left[\frac{\pi}{\alpha} \mathrm{Tr}\, \mathcal{G}(\mathbf{k})\right]\right] \ .
\end{aligned} \qquad \text{(E9)}
$$

In the above formulas, N represents the number of sites in $\mathcal{L}^D$, and Ω is the area of the Wigner-Seitz cell on $\mathcal{L}$; the trace over $\mathcal{G}(\mathbf{k})$ is with respect to internal basis indices, which are present if the lattice is not a Bravais lattice. The spin-wave system does not exhibit critical behavior at any finite value of the coupling α. All the interesting physics lie in the vortex-gas piece,

$$
\begin{aligned}
H_{\mathrm{VG}} &= \frac{\pi^2}{\alpha} \sum_{i,j} (m_i - f_i) \mathcal{G}_{ij} (m_j - f_j) \ , \\
Z_{\mathrm{VG}} &= \mathrm{Tr}\, e^{-H_{\mathrm{VG}}} \ .
\end{aligned} \qquad \text{(E10)}
$$

Now $\mathcal{G}_{ij}$ is divergent, and it is customary to identify the finite difference $G_{ij} \equiv 2\pi(\mathcal{G}_{ii} - \mathcal{G}_{ij})$. The divergence of $\mathcal{G}_{ii}$ manifests itself in a "neutral vorticity" constraint, as it is easy to show that only neutral configurations (i.e., those which satisfy $Q[m] \equiv \sum_i (m_i - f_i) = 0$) have nonzero Boltzmann weight in the partition sum. This leads one to the following result:

$$
H_{\mathrm{VG}} = -\frac{\pi}{2\alpha} {\sum_{i,j}}' (m_i - f_i) G_{ij} (m_j - f_j) \ . \qquad \text{(E11)}
$$

Note that the above derivation allows for nonuniform flux f_k per plaquette.

APPENDIX F: RING EXCHANGE AND MAGNETOPHONONS

As discussed in the body of this chapter, density fluctuations in the $\alpha < \alpha_c$ phase interact via a logarithmic potential. Treated in the harmonic approximation, the main effect of this result is to alter the $\omega_k \propto k^{3/2}$ form of the magnetophonon dispersion, and, in the simplest scheme possible, a linear spectrum results. In this appendix, we shall discuss the details of this calculation.

1. Maki-Zotos revisited

Maki and Zotos[8] found that the Hartree-Fock charge-density wave calculations could be reproduced accurately by the simple ansatz wave function

$$
|\Psi\rangle = (N!)^{-1/2} \sum_{\sigma \in s_N} |\mathbf{R}_{\sigma(1)}, \mathbf{R}_{\sigma(2)}, \ldots, \mathbf{R}_{\sigma(N)}\rangle \ . \qquad \text{(F1)}
$$

The Maki-Zotos (MZ) state is just a determinant formed of single-particle coherent states centered on the sites of a triangular lattice $\mathbf{R}_i = \mathbf{T}_i$. The ground-state energy is then evaluated according to

$$
\begin{aligned}
E_0 &= \frac{e^2}{\epsilon} \left\langle \Psi \left| \sum_{j<k} \frac{1}{|\mathbf{r}_{jk}|} \right| \Psi \right\rangle \Big/ \langle \Psi | \Psi \rangle \\
&= \sum_{j<k} V_2(\mathbf{R}_j - \mathbf{R}_k) + \sum_{i<j<k} V_3(\mathbf{R}_i, \mathbf{R}_j, \mathbf{R}_k) + \cdots \ .
\end{aligned} \qquad \text{(F2)}
$$

Magnetophonons may be investigated by letting the guiding centers deviate from the lattice sites, e.g., $\mathbf{R}_i \to \mathbf{T}_i + \mathbf{u}_i$. Working within the harmonic approximation, and in addition neglecting all contributions from three-body terms, etc., the "bare" magnetophonon Hamiltonian becomes

$$
\begin{aligned}
H^0_{\mathrm{mp}} &= \delta^2 E_0[\{\mathbf{u}_i\}] \\
&= \tfrac{1}{2} \sum_{\mathbf{k}} \Phi_{ij}(\mathbf{k}) u_i(\mathbf{k}) u_j(-\mathbf{k}) \ , \\
\Phi_{ij}(\mathbf{k}) &= \frac{\nu}{2\pi l^2} \sum_{\mathbf{G}} [(k_i + G_i)(k_j + G_j) V(\mathbf{k}+\mathbf{G}) \\
&\qquad - G_i G_j V(\mathbf{G})] \ ,
\end{aligned} \qquad \text{(F3)}
$$

where we have suppressed the label "2" on V_2, and where subscripts on nonboldface variables index a Cartesian component, and are not to be confused with particle label subscripts.

The dynamics behind the Hamiltonian of Eq. (F3) are concealed in the projection to the lowest Landau level in which the cyclotron motion of the $\mathbf{u}_i$ variables is quenched. The resulting Hamiltonian can be written in terms of the noncommuting guiding center variables. Using complex coordinates $z_i = u_{i,x} + i u_{i,y}$,

$$z_k=\frac{1}{\sqrt{N}}\sum_i E^{-i\mathbf{k}\cdot\mathbf{T}_i}z_i=l\sqrt{2}(a_k+b^\dagger_{-k})\ ,$$
$$z^*_{-k}=\frac{1}{\sqrt{N}}\sum_i e^{-i\mathbf{k}\cdot\mathbf{T}_i}\bar{z}_i=l\sqrt{2}(a^\dagger_{-k}+b_k)\ , \tag{F4}$$

one obtains the magnetophonon Hamiltonian

$$H^0_{\rm mp}=\sum_{\mathbf{k}}[\chi(\mathbf{k})b^\dagger_k b_k+\chi(\mathbf{k})b^\dagger_{-k}b_{-k}+\varphi(\mathbf{k})b_k b_{-k}+\varphi^*(\mathbf{k})b^\dagger_k b^\dagger_{-k}]\ , \tag{F5}$$

where

$$\chi(\mathbf{k})=\tfrac{1}{2}l^2[\Phi_{xx}(\mathbf{k})+\Phi_{yy}(\mathbf{k})]\ ,$$
$$\varphi(\mathbf{k})=\tfrac{1}{2}l^2[\Phi_{xx}(\mathbf{k})-\Phi_{yy}(\mathbf{k})+2i\Phi_{xy}(\mathbf{k})]\ . \tag{F6}$$

$H^0_{\rm mp}$ can be diagonalized by a Bogoliubov transformation with the result that the bare magnetophonon branch is given by

$$\omega^0_k=[\,|\chi(\mathbf{k})|^2-|\varphi(\mathbf{k})|^2]^{1/2}\ . \tag{F7}$$

In the long-wavelength limit, $\Phi_{ij}(\mathbf{k})$ tends to the continuum result,

$$\Phi_{ij}(\mathbf{k})=\frac{\nu e^2}{\epsilon l}\{[U(kl)+C_0]k_ik_j+C_1k^2\delta_{ij}+O(k^3)]\}\ ,$$
$$C_0=\tfrac{1}{8}\sum_{\mathbf{G}\neq 0}[8U(Gl)+7(Gl)U'(Gl)+(Gl)^2U''(Gl)]\ ,$$
$$C_1=\tfrac{1}{16}\sum_{\mathbf{G}\neq 0}[3(Gl)U'(Gl)+(Gl)^2U'(Gl)]\ , \tag{F8}$$

where $\mathbf{G}$ is a reciprocal lattice vector, and where we have defined the dimensionless potential $U(ql)$ by

$$V(q)\equiv\frac{2\pi e^2 l}{\epsilon}U(ql)\ . \tag{F9}$$

The MZ potential,

$$V(\mathbf{R})=\frac{\sqrt{\pi}e^2}{4\epsilon l}\,\mathrm{sech}(R^2/8l^2)I_0(R^2/8l^2)\ , \tag{F10}$$

differs from the projected Coulomb form of Eq. (D1) in its short-wavelength behavior—this is a consequence of the exchange corrections introduced by antisymmetrization of the MZ wave function. Maki and Zotos found that, whereas the total energy is adequately represented by the Hartree term throughout the range $0<\nu\lesssim 0.4$, the shear modulus C_1, and hence the magnetophonon spectrum, is quite sensitive to the effects of the two-particle antisymmetrization inherent in Eq. (F10). The Fourier components of the Fock-corrected potential are given by

$$U(ql)=\frac{1}{ql}e^{-q^2l^2}+\sum_{n=1}^{\infty}(-1)^nU_n(ql)\ ,$$
$$U_n(ql)=\frac{\sqrt{\pi}}{\sqrt{n(n+1)}}\exp\left[-\frac{1}{2}\left[\frac{2n+1}{n(n+1)}\right]q^2l^2\right]\times I_0\left[\frac{q^2l^2}{2n(n+1)}\right]\ . \tag{F11}$$

2. Ring-exchange effects

We begin with the effective Hamiltonian of Eq. (4.8), obtained by tracing over the ring-exchange variables in the presence of a phonon field:

$$H_{\rm eff}=\frac{\pi^2}{\alpha\tau_0}(2\pi l^2)^{-2}\sum_{\mathbf{k}}\delta A_\mu(\mathbf{k})\left[\mathcal{G}_{\mu\nu}(\mathbf{k})-\frac{2\pi^2}{\alpha}\mathcal{G}_{\mu\lambda}(\mathbf{k})Q_{\lambda\lambda'}(\mathbf{k})\mathcal{G}_{\lambda'\nu}(\mathbf{k})\right]\delta A_\nu(-\mathbf{k})\ . \tag{F12}$$

In the above expression, the Greek subscripts refer to basis elements of the plaquette lattice ($\mu=1$ for upward-pointing triangles, $\mu=2$ for downward-pointing triangles, and summation convention employed for these indices). One finds that the Fourier component of the area fluctuation is given by

$$\delta A_\mu(\mathbf{T})=\frac{1}{\sqrt{N}}\sum_{\mathbf{k}}e^{i\mathbf{k}\cdot\mathbf{T}}\delta A_\mu(\mathbf{k})$$
$$=\frac{1}{\sqrt{N}}\sum_{\mathbf{k}}e^{i\mathbf{k}\cdot\mathbf{T}}[B_\mu(\mathbf{k})b_{\mathbf{k}}+B^*_\mu(-\mathbf{k})b^\dagger_{-\mathbf{k}}]+\frac{1}{N}\sum_{\mathbf{k},\mathbf{k}'}e^{i(\mathbf{k}-\mathbf{k}')\cdot\mathbf{T}}[D_\mu(\mathbf{k},\mathbf{k}')b^\dagger_{-\mathbf{k}}b_{-\mathbf{k}'}+D^*_\mu(-\mathbf{k},-\mathbf{k}')b^\dagger_{\mathbf{k}}b_{\mathbf{k}}]\ , \tag{F13}$$

with

$$B_1(\mathbf{k})=\frac{\sqrt{2}l}{4i}[T_2(e^{i\mathbf{k}\cdot\mathbf{T}_1}-1)+T_1(1-e^{i\mathbf{k}\cdot\mathbf{T}_2})]\ ,$$
$$B_2(\mathbf{k})=\frac{\sqrt{2}l}{4i}[T_2e^{i\mathbf{k}\cdot\mathbf{T}_2}(e^{i\mathbf{k}\cdot\mathbf{T}_1}-1)+T_1e^{i\mathbf{k}\cdot\mathbf{T}_1}(1-e^{i\mathbf{k}\cdot\mathbf{T}_2})]\ , \tag{F14}$$
$$D_1(\mathbf{k},\mathbf{k}')=\frac{2l^2}{4i}(1-e^{i\mathbf{k}\cdot\mathbf{T}_2})(1-e^{i\mathbf{k}'\cdot\mathbf{T}_1})\ ,$$
$$D_2(\mathbf{k},\mathbf{k}')=\frac{2l^2}{4i}(1-e^{i\mathbf{k}\cdot\mathbf{T}_2})(1-e^{-i\mathbf{k}'\cdot\mathbf{T}_1})e^{i\mathbf{k}\cdot\mathbf{T}_1}e^{-i\mathbf{k}'\cdot\mathbf{T}_2}\ ,$$

and where $\mathbf{T}_1$, $\mathbf{T}_2$, T_1, and T_2 are vector and complex representations of the two primitive direct lattice vectors $\mathbf{T}_{1,0}$ and $\mathbf{T}_{0,1}$, respectively. The triangular lattice Green function is written

$$\mathcal{G}(\mathbf{k})=\frac{\begin{pmatrix}3 & 1+e^{i\mathbf{k}\cdot\mathbf{T}_1}+e^{i\mathbf{k}\cdot\mathbf{T}_2}\\ 1+e^{-i\mathbf{k}\cdot\mathbf{T}_1}+e^{-i\mathbf{k}\cdot\mathbf{T}_2} & 3\end{pmatrix}}{\{6-2\cos(\mathbf{k}\cdot\mathbf{T}_1)-2\cos(\mathbf{k}\cdot\mathbf{T}_2)-2\cos[\mathbf{k}\cdot(\mathbf{T}_1-\mathbf{T}_2)]\}}\ . \tag{F15}$$

Now only the lowest-order terms at small k are investigated. This approximation involves neglecting the $Q_{\mu\nu}(\mathbf{k})$ contribution to the effective interaction (valid in the long-wavelength limit when α is less than α_c), and retaining only terms bilinear in the operators b and $b^\dagger$:

$$H_{\rm eff}=\sum_{\mathbf{k}}[\lambda(\mathbf{k})b_k^\dagger b_k+\lambda(\mathbf{k})b_{-k}^\dagger b_{-k}+\psi(\mathbf{k})b_k b_{-k}+\psi^*(\mathbf{k})b_k^\dagger b_{-k}^\dagger],$$

$$\lambda(\mathbf{k})=\frac{\pi^2}{2\alpha\tau_0}(2\pi l^2)^{-2}[B_\mu(\mathbf{k})\mathcal{G}_{\mu\nu}(\mathbf{k})B_\nu^*(\mathbf{k})+B_\mu^*(-\mathbf{k})\mathcal{G}_{\mu\nu}(-\mathbf{k})B_\nu(-\mathbf{k})], \tag{F16}$$

$$\psi(\mathbf{k})=\frac{\pi^2}{2\alpha\tau_0}(2\pi l^2)^{-2}[B_\mu(\mathbf{k})\mathcal{G}_{\mu\nu}(\mathbf{k})B_\nu(-\mathbf{k})+B_\mu(-\mathbf{k})\mathcal{G}_{\mu\nu}(-\mathbf{k})B_\nu(\mathbf{k})].$$

The complete magnetophonon Hamiltonian is then given by the sum of $H_{\rm eff}$ and $H^0_{\rm mp}$. In the long-wavelength limit, where

$$\lambda(\mathbf{k})\to\frac{\sqrt{3}\pi}{4\alpha\tau_0},\qquad \psi(\mathbf{k})\to\frac{\sqrt{3}\pi}{4\alpha\tau_0}\left[\frac{k_x+ik_y}{k}\right]^2, \tag{F17}$$

the phonon spectrum takes the acoustic form $\omega_k=ck$, where the "sound" velocity is

$$c=\left[\frac{e^2}{\epsilon l}\frac{\sqrt{3}\pi\nu}{\alpha\tau_0}C_1\right]^{1/2}. \tag{F18}$$

---

*Present address: State University of New York, Stony Brook, NY 11974.

†Present address: McMaster University, Hamilton, Ontario, Canada L8S 4M1.

‡Present address: James Franck Institute, 5640 S. Ellis Ave., Chicago, IL 60637.

[1]K. von Klitzing, G. Dorda, and M. Pepper, Phys. Rev. Lett. **45**, 494 (1980).

[2]D. C. Tsui, H. L. Störmer, and A. C. Gossard, Phys. Rev. Lett. **48**, 1559 (1982).

[3]D. Yoshioka, B. I. Halperin, and P. A. Lee, Phys. Rev. Lett. **50**, 1219 (1983).

[4]B. I. Halperin, Helv. Phys. Acta **56**, 75 (1983).

[5]H. Fukuyama, P. M. Platzman, and P. W. Anderson, Phys. Rev. B **19**, 5211 (1979).

[6]D. Yoshioka, Phys. Rev. B **27**, 3637 (1983).

[7]D. Yoshioka and P. A. Lee, Phys. Rev. B **27**, 4986 (1983).

[8]Kazumi Maki and Xenophon Zotos, Phys. Rev. B **28**, 4349 (1983).

[9]R. B. Laughlin, Phys. Rev. Lett. **50**, 1395 (1983).

[10]F. D. M. Haldane, Phys. Rev. Lett. **51**, 605 (1983).

[11]S. A. Trugman and S. Kivelson, Phys. Rev. B **31**, 5280 (1985).

[12]W. P. Su, J. R. Schrieffer, and A. J. Heeger, Phys. Rev. Lett. **42**, 1698 (1979).

[13]Daniel Arovas, J. R. Schrieffer, and Frank Wilczek, Phys Rev. Lett. **53**, 722 (1984).

[14]B. I. Halperin, Phys. Rev. Lett. **52**, 1583 (1984).

[15]F. D. M. Haldane and E. H. Rezayi, Phys. Rev. Lett. **54**, 237 (1985).

[16]F. D. M. Haldane, Phys. Rev. Lett. **55**, 2095 (1985).

[17]Daijiro Yoshioka, Phys. Rev. B **29**, 6833 (1984).

[18]S. M. Girvin, A. H. MacDonald, and P. M. Platzman, Phys. Rev. Lett. **54**, 581 (1985); S. M. Girvin, A. H. MacDonald, and P. M. Platzman, Phys. Rev. B **33**, 2481 (1986).

[19]R. P. Feynman, Phys. Rev. **91**, 1291 (1953); **91**, 1301 (1953); R. P. Feynman and M. Cohen, Phys. Rev. **102**, 1189 (1956).

[20]R. B. Laughlin, Surf. Sci. **142**, 163 (1984).

[21]S. M. Girvin and A. H. MacDonald (unpublished).

[22]G. Baskaran (unpublished).

[23]D. J. Thouless, Phys. Rev. B **31**, 8305 (1985).

[24]Steven Kivelson, C. Kallin, Daniel P. Arovas, and J. R. Schrieffer, Phys. Rev. Lett. **56**, 873 (1986).

[25]G. Baskaran, Phys. Rev. Lett. **56**, 2716 (1986).

[26]L. Schulman, *Techniques and Applications of Path Integration* (Wiley, New York, 1981), Chap. 27.

[27]John R. Klauder, in *Path Integrals and Their Applications in Quantum, Statistical, and Solid State Physics,* Vol. 34 of *NATO Advanced Study Institutes, Series B: Physics,* edited by George Papadopoulos and J. T. Devreese (Plenum, New York, 1978).

[28]Jainendra Jain and Steven Kivelson (unpublished).

[29]For a general path, there may also be contributions to the imaginary part of the action from terms such as $\dot{R}_j''\wedge R_j''$. These contributions can be treated in the same way as the deviations from straight line segments, and also lead to a renormalization of α_0.

[30]R. Rajaraman, *Solitons and Instantons* (North-Holland, Amsterdam, 1982).

[31]S. T. Chui and J. D. Weeks, Phys. Rev. B **14**, 4978 (1976).

[32]Robert H. Swendsen, Phys. Rev. Lett. **37**, 1478 (1976).

[33]W. J. Shugard, J. D. Weeks, and G. H. Gilmer, Phys. Rev. Lett. **41**, 1399 (1978).

[34]S. Teitel and C. Jayaprakash, Phys. Rev. B **27**, 598 (1983).

[35]Wan Y. Shih and D. Stroud, Phys. Rev. B **28**, 6575 (1983).

[36]S. Teitel and C. Jayaprakash, Phys. Rev. Lett. **51**, 1999 (1983).

[37]Wan Y. Shih and S. Stroud, Phys. Rev. B **30**, 6774 (1984).

[38]Thomas C. Halsey, Phys. Rev. B **31**, 5728 (1985); J. Phys. C **18**, 2437 (1985).

[39]J. Tobochnik and G. V. Chester, Phys. Rev. B **20**, 3761 (1979).

[40]See Ref. 37 for transition temperatures on triangular and honeycomb lattices. One can also estimate α_c for different lattices by multiplying the calculated value for one lattice by a mean-field-type ratio of lattice coordination numbers.

[41]J. M. Caillol, D. Levesque, J. J. Weis, and J. P. Hansen, J. Stat. Phys. **28**, 2 (1985).

[42]J. M. Kosterlitz and D. J. Thouless, J. Phys. C **6**, 1181 (1973).

[43]R. P. Feynman, *Statistical Mechanics* (Benjamin, New York, 1972).

[44]Jorge V. José, Leo P. Kadanoff, Scott Kirkpatrick, and David R. Nelson, Phys. Rev. B **16**, 1217 (1977).

[45]Lynn Bonsall and A. A. Maradudin, Phys. Rev. B **15**, 1959 (1977).
[46]H. L. Störmer, A. Chang, D. C. Tsui, J. C. M. Hwang, A. C. Gossard, and W. Wiegmann, Phys. Rev. Lett. **50**, 1953 (1983).
[47]D. Lee (private communications).
[48]D. Lee, G. Baskaran, and S. Kivelson (unpublished).
[49]S. M. Girvin and A. H. MacDonald (unpublished).
[50]D. J. Thouless, Proc. R. Soc. London **86**, 893 (1965).
[51]S. M. Girvin and Terrence Jach, Phys. Rev. B **29**, 5617 (1984).